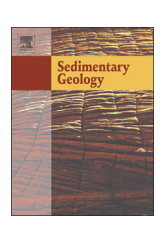
FISEVIER

Contents lists available at ScienceDirect

Sedimentary Geology

journal homepage: www.elsevier.com/locate/sedgeo



The Whale Point Formation: A stratigraphic record of high-frequency climate and sea-level fluctuations in the Bahamas during Marine Isotope Stage 5a (ca. 80 ka BP)



Pascal Kindler a,*, Paul J. Hearty b

- ^a Department of Earth Sciences, University of Geneva, Rue des Maraîchers 13, 1205 Geneva, Switzerland
- ^b Department of Geological Sciences, Jackson School of Geosciences, The University of Texas at Austin, USA

ARTICLE INFO

Article history: Received 5 November 2021 Received in revised form 16 February 2022 Accepted 17 February 2022 Available online 26 February 2022

Editor: Dr. Brian Jones

Keywords: Bahamas Pleistocene Climate Sea-level Eolianites Stratigraphy

ABSTRACT

In this paper, we formally define a series of bioclastic eolianites and protosols exposed on high-energy bank margins throughout the Bahamas archipelago as the Whale Point Formation (WPF). The position of this new lithostratigraphic unit above and seaward of deposits dated to Marine Isotope Stage (MIS) 5e and below Holocene sediments constrains its age to the latest Pleistocene, more precisely to MIS 5a (ca. 88–74 ka BP). This age is further corroborated by amino-acid racemization data calibrated with U—Th ages. Based on their sedimentological characteristics, the WPF eolianites are interpreted as landward-advancing dunes decoupled from their source beaches. Relying on the faunal content, the maximum elevation of relative sea level during MIS 5a can be roughly estimated at ca. 9 ± 2 m below the present stand. The WPF includes two phases of eolian deposition separated by an interval of negative sediment budget and pedogenesis. These different facies possibly reflect millennial-scale sea-level and climate instability during MIS 5a, the latter being likely related to shifts in the mean annual position of the intertropical convergence zone and associated rainfall belt.

© 2022 The Author(s). Published by Elsevier B.V. This is an open access article under the CC BY-NC-ND license (http://creativecommons.org/licenses/by-nc-nd/4.0/).

1. Introduction

Reconstructing the history of climate and sea-level changes during the Quaternary is of prime importance for better addressing potential anthropogenic climate changes. To unravel this history, we investigate the record of shallow-water tropical carbonates because of their sensitivity to subtle environmental fluctuations (e.g., Lees and Buller, 1972; Mutti and Hallock, 2003; James and Jones, 2015 and references therein), their ability to preserve past sea-level indicators due to rapid cementation (Dravis, 1996; Friedman, 1998; Kindler and Mazzolini, 2001), and their accessibility to multiple dating methods (e.g., Hearty and Kaufman, 2000; Thompson et al., 2011). Further, peritidal limestones from tectonically quiescent areas, such as the Bahamas, are particularly suitable for assessing ancient sea-level markers because the elevation uncertainties related to subsidence or uplift rates are minimal at these locations.

However, because the geology of these carbonate islands is relatively complex (e.g., Garrett and Gould, 1984; Hearty and Kindler, 1993a and 1993b, 1997; Carew and Mylroie, 1995a, 1997; Hearty, 1998; Godefroid, 2012; Dravis and Wanless, 2017; Kerans et al., 2019), correlating

E-mail address: Pascal.Kindler@unige.ch (P. Kindler).

depositional phases to specific sea-level events is not always a straightforward task. A case in point is the stratigraphic record from the Late Pleistocene (i.e., Marine Isotope Stage [MIS] 5; ca. 132-74 ka BP; Railsback et al., 2015). This time interval encompasses several sedimentation episodes represented by reefal, shoreface and foreshore deposits, as well as by eolianites of both skeletal and oolitic composition. One school of thought (e.g., Carew and Mylroie, 1995a, 1997, 2001; Mylroie, 2008; Yanes and Romanek, 2013; Martin et al., 2020) considers that all these sediments were accumulated during the last interglacial period (LIG, MIS 5e, ca. 132-118 ka BP; Railsback et al., 2015), whereas the other (e.g., Hearty and Kindler, 1993a and 1993b; Kindler and Hearty, 1995, 1996, 1997; Hearty, 1998; Godefroid, 2012; Jackson, 2017; Vimpere, 2017; Godefroid et al., 2019) correlates part of this record, namely the skeletal eolianites, to MIS 5a (ca. 88–74 ka BP; Railsback et al., 2015). On San Salvador Island, Hearty and Kindler (1993a) coined the term Almgreen Cay Formation (ACF) for these eolianites, which actually corresponded to a morphostratigraphic unit, i.e., a body of rock essentially defined by its surface form and lithology (Bowen, 1988).

In this paper, we officially rename, redefine, and supplant the ACF as the *Whale Point Formation* (WPF) based on more than 30 years of geological investigations across the Bahamian archipelago. The two objectives of this study are thus: (1) to formally describe the WPF as a lithostratigraphic unit, and (2) to address the implications of the

^{*} Corresponding author at: Ferme du Terril, 17 route des Tavernes, 1610 Châtillens, Switzerland.

recognition of this formation as a record of climate and sea level during MIS 5a

2. Geographic and geological setting of the Bahamas

The Bahamas archipelago, including the Turks and Caicos islands, extends for nearly 1000 km (ca. 7° of latitude) in the northwestern Atlantic Ocean (Fig. 1). It stands on the passive southeastern margin of the North American plate, but is fairly close to the (active) northern Caribbean plate boundary zone. This region has long been considered as tectonically stable, and only affected by slow subsidence related to sedimentary loading (ca. 2 cm/kyr in the northern Bahamas since the Oligocene; Lynts, 1970). More recent studies (Mullins and Van Buren, 1981; Masaferro and Eberli, 1999; Kindler et al., 2011; Mulder et al., 2012), however, suggest that the area has been affected by several tectonic episodes during the Neogene and even in the Quaternary.

The archipelago consists of a series of flat-topped, steep-sided carbonate platforms (i.e., banks) separated by deep channels (Fig. 1). Its northeastern part essentially comprises two large edifices (Little Bahama Bank and Great Bahama Bank) that are largely flooded, and bear elongated, low-elevation islands, mostly on their eastern (windward) sides (e.g., Abaco, Eleuthera). Its southeastern portion shows several smaller banks that are only marginally submerged, and often capped by relatively large islands (e.g., Mayaguana and Great Inagua banks). This morphological difference is likely due to increasing tectonic influence towards the south (Mullins et al., 1991, 1992). Except for Cay Sal Bank (Fig. 1; Hine and Steinmetz, 1984), water depth seldom exceeds 8 to 12 m on the flooded parts of the bank tops (e.g., Harris et al., 2015). The platform margins represent gently sloping (3 to 20°; Wilber et al., 1990; Grammer et al., 1991; Rankey and Doolittle, 2012) intervals between the platform interior and the bank edges (i.e., the greatest seaward increase in gradient; Playton et al., 2010) which occur at 20 to 60 m below sea level (Bergman et al., 2010), and generally tower above sub-vertical escarpments. The width of the platform margins varies from a few 100's of m to up to 4 km along the windward and leeward sides of the banks, respectively (Wilber et al., 1990; Jackson, 2017).

The largest part of Bahamas region is located in the tropical savanna climate zone of the Köppen-Geiger classification (*Aw*; Beck et al., 2018). The northern (e.g., Abaco) and the southern portions (e.g., Great Inagua, eastern Mayaguana) of the archipelago are respectively positioned in the tropical monsoon (*Am*) and hot steppe climate zones (*Bsh*; Beck et al., 2018). All areas experience two main seasons largely determined by the movements of the Atlantic Intertropical Convergence Zone (ITCZ). In the winter, the southward motion of the ITCZ induces temperate-warm and dry conditions over the archipelago with prevailing NE trade winds and cold western fronts. By contrast, in the summer, its northward shift results in a hot and humid climate with weaker trade winds from the E and SE (Zhuravleva and Bauch, 2018). The average yearly rainfall is ca. 850 mm, but regional variations range from 660 mm to 1450 mm/yr (Sealey, 2006).

The ca. 700 islands and cays of the Bahamas consist of vertically stacked and/or laterally juxtaposed carbonate units, mostly eolianites, separated by thin red to brown layers generally corresponding to terra-rossa paleosols. The latter are composed of a mix of carbonates and of an insoluble clay fraction primarily derived from atmospheric aerosols (Muhs et al., 1990; Nawratil de Bono, 2008). Relying on a depositional model developed in Bermuda (Bretz, 1960; Vacher, 1973), Carew and Mylroie (1995a, 2001) surmised that carbonate sediments accumulate during interglacial highstands of sea level, when the platform tops are flooded by a shallow water layer, and that paleosols mostly form during lowstands, when the banks are exposed. They further envisioned three phases of eolianite deposition related to their time of origin during a highstand. These phases, labeled "transgressive", "stillstand" and "regressive", correspond to the early part, the acme and the late part of the flooding event, respectively. In this model, eolianites of all phases are closely tied to their source beaches.

Stratigraphic research on the Bahamas islands began in the early 1980's with the landmark paper of Garrett and Gould (1984) on New

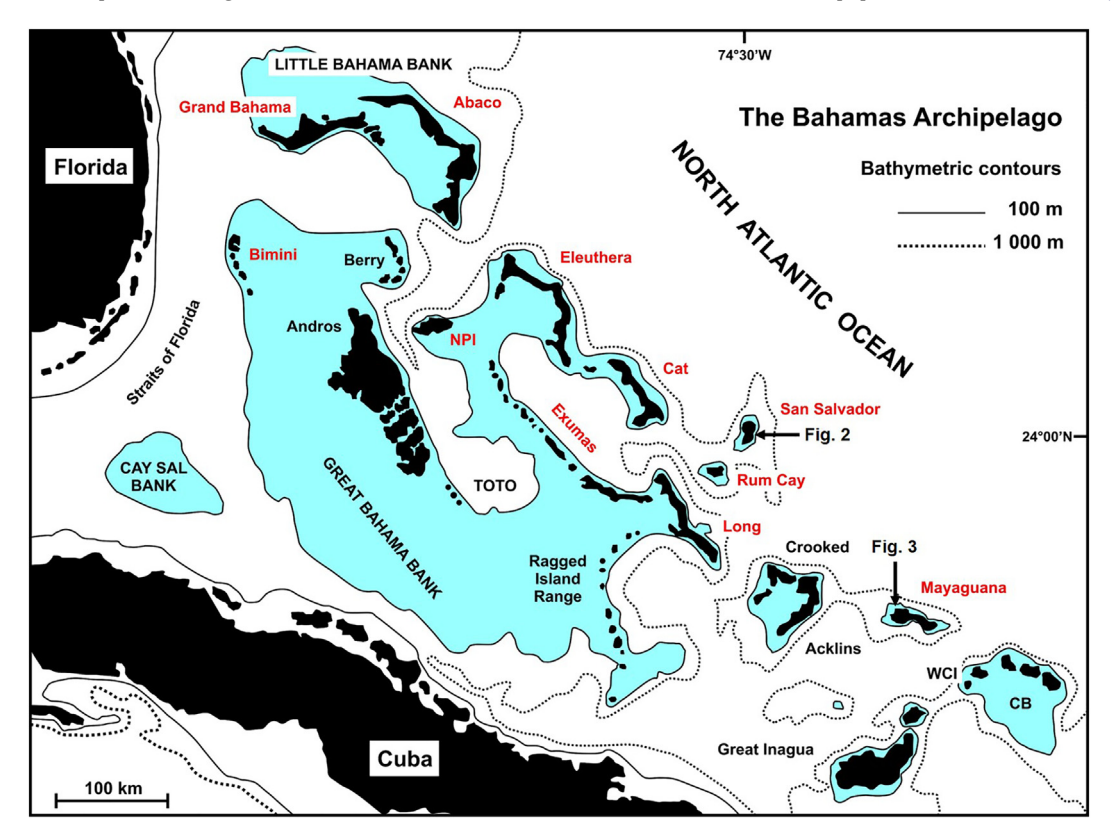


Fig. 1. Location map of the Bahamas archipelago. NPI = New Providence Island; TOTO = Tongue of the Ocean; WCI = West Caicos Island; CB = Caicos Bank. Islands designated with red characters bear exposures of the Whale Point Formation.

Providence. Around that time, three allostratigraphic units were defined by Carew and Mylroie (1985) on San Salvador: the Owl's Hole, the Grotto Beach, and the Rice Bay formations (Table 1). Carew and Mylroie's (1985) stratigraphic scheme was largely maintained by its authors during the next two decades while concurrent investigations on other islands (e.g., Hearty and Kindler 1993a and 1993b, 1997; Kindler and Hearty, 1995, 1996, 1997; Hearty, 1998; Kindler, 1995) identified six carbonate-paleosol "couplets" (Hearty and Kaufman, 2000), spanning a time interval from the Middle Pleistocene (MIS 13) to the Holocene. More recently, geological research on Mayaguana and Crooked islands revealed the occurrence of rock units predating the Middle Pleistocene, and going as far back as the Early Miocene (Fig. 2, Table 1; Kindler et al., 2011; Godefroid, 2012; Godefroid and Kindler, 2016; Godefroid et al., 2019).

3. Methods

Over the years, we used a multi-method approach to unravel the stratigraphy of the Bahamas islands including morphostratigraphy, stratigraphy, sedimentology and quantitative petrographic analysis, as well as amino-acid racemization, U-series, ⁸⁷Sr/⁸⁶Sr, and ¹⁴C dating. The methods specifically pertaining to the recognition of the WPF are briefly described below.

3.1. Morphostratigraphy

Prior to fieldwork, we evaluated the morphostratigraphy on topographic maps and air photos applying the principles of lateral accretion (Itzhaki, 1961; Vacher, 1973) and catenary growth (Garrett and Gould, 1984). The former states that, on a prograding shoreline, deposits

become younger seaward. The latter principle, which is an exception to the first one, asserts that catenary ridges are younger than their anchoring headlands (Fig. 2 in Kindler and Hearty, 1996).

3.2. Stratigraphy and sedimentology

Measured sections were established at 28 sites on 11 islands (Fig. 1). When exposed, boundaries with underlying and overlying stratigraphic units were scrutinized in details. Physical and biogenic sedimentary structures were examined in the field to obtain information about depositional settings and, eventually, past sea-level elevation.

3.3. Petrography

Following examination in the field, selected samples were collected from the studied sections, impregnated with blue epoxy resin, thinsectioned and observed under a polarizing microscope. Carbonate minerals were identified by staining techniques (Miller, 1988), and quantitative petrographic analysis was made with a SWIFT automatic point-counter (model F). The applied analytical method is thoroughly described in Kindler and Hearty (1996).

3.4. Amino-acid racemization (AAR) dating

AAR dating was used on whole-rock samples for correlating units within and between islands, and determining their relative ages. The method relies on the slow interconversion (racemization) of L-amino acids, within indigenous proteins preserved in the sample, to increasing proportions of their respective D-configurations until an equilibrium mixture of D- and L-amino acids is attained. This study utilized the

Table 1
Chart representing the most important stratigraphic schemes proposed for the Quaternary of the Bahamas in the past 35 years. * Dixon Hill Mb.: Carew and Mylroie (1985) attributed the rocks exposed at Dixon Hill (San Salvador) to MIS 5a, but later withdrew this term from the stratigraphic literature (Carew and Mylroie, 1995a). This rock body was correlated to the Middle Pleistocene by Hearty and Kindler (1993a). **Owl's Hole Fm.: based on paleomagnetic data, Carew and Mylroie (1985) first placed this formation in the Early Pleistocene. Additional measurements made a few years later (Carew and Mylroie, 1995a) forced these authors to replace this unit in the Middle Pleistocene.

EPOCHS	MIS	Carew & Mylroie (1985) San Salvador		Hearty & Kindler (1993) San Salvador		Carew & Mylroie (1995) The Bahamas		Hearty & Kaufman (2000) The Bahamas	Kindler et al. (2010) The Bahamas		Godefroid (2012) Mayaguana		Kerans et al (2019) West Caicos	
HOLOCENE	1	Rice Bay Fm.	Hanna Bay Mb. E. A. S.	-1	East Bay Mb.	Rice Bay Fm.		Couplet VI	Rice Bay Fm.					
				Вау Еп	Hanna Bay Mb.		Hanna Bay Mb.			Hanna Bay Mb.		Rice Bay Fm.	Long Road Unit	
			North Point Mb.	Rice	North Point Mb.		North Point Mb.			North Point Mb.			NOT IDENTIFIED	
LATE PLEISTOCENE	5a		Dixon Hill Mb. *		Almgreen Cay Fm.		IOT IDENTIFIED	Couplet V	١	Whale Point Fm.		Whale Point Fm.	NOT IDENTIFIED	
	5e	Grotto Beach Fm.	Cockburn Town Mb.	Fm.	Fernandez Bay Mb.				Fm.	Cockburn Town	Fm.	Big Cove Mb.	NE Ridge Unit	
				each	Cockburn Town	Cockburn Town Mb.		Couplet IV	Beach Fm.	Mb.	Beach Fm.	Cockburn Town	Boat Cove Unit	
				tto B	Mb.			обарысту	Grotto B		tto B	Mb.	South Reef Unit	
			French Bay Mb.	Gro	French Bay Mb.	ı	French Bay Mb.			French Bay Mb.	Grotto	French Bay Mb.	Railroad Ridge Unit	
MIDDLE PLEISTOCENE	7				Fortune Hill Fm.			Couplet III						
	9	-		Owl's Hole Fm.		Owl's Hole Fm.		Couplet III	Owl's Hole Fm.		Owl's Hole Fm.		Star Town Unit	
	11							Couplet II						
	>13				OWIS HOIE FM.			Couplet I						
CALABRIAN	19			NOT IDENTIFIED		NOT IDENTIFIED			Misery Point Fm.		Misery Point Fm.			
	63	Owl's Hole Fm. **						NOT IDENTIFIED					NOT IDENTIFIED	

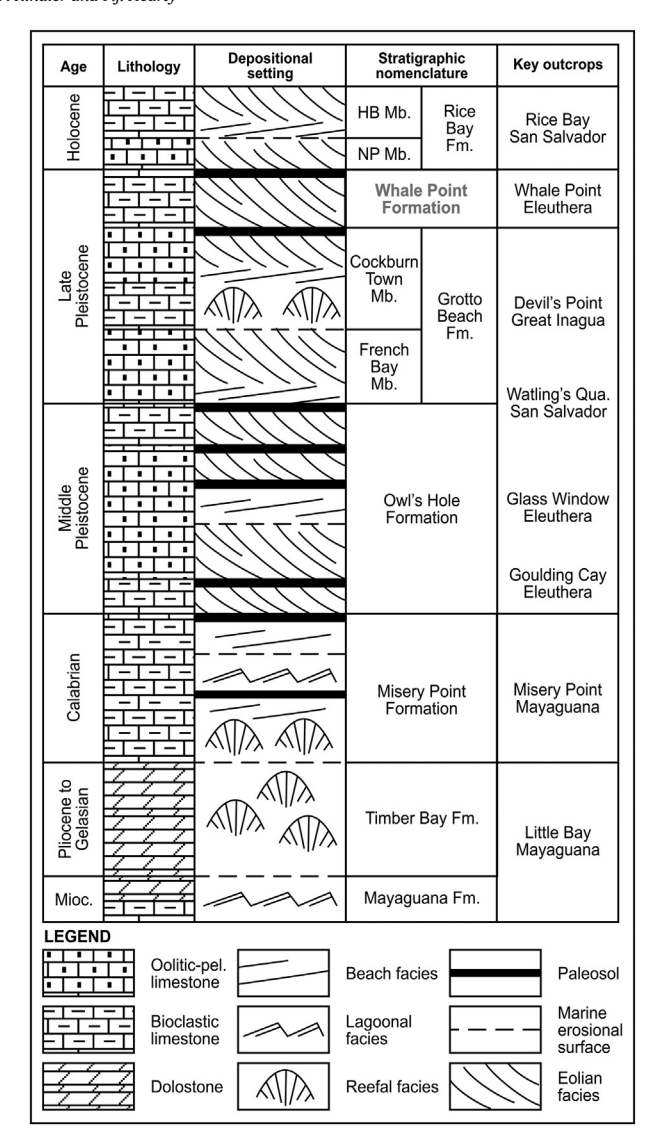


Fig. 2. Synthetic stratigraphic log of the Bahamas islands (modified from Kindler et al., 2010). Mb = member; Fm. = formation; Qua = quarry; Mioc. = Miocene; pel. = peloidal; HB = Hanna Bay; NP = North Point.

ratio of the stereoisomers of isoleucine (D-alloisoleucine/L-isoleucine or A/I ratio). The A/I ratio is zero in most living tissues (D-alloisoleucine is not present), and approaches an equilibrium value of 1.3 at an exponentially decreasing rate depending on the time elapsed since the death of the constituent organisms and the temperature history of the sedimentary deposit. All samples were sent for analysis to the Amino Acid Geochronology Laboratory of the Northern Arizona University. Prior to 2013, A/I ratios were directly measured with the traditional, labor intensive, ion-exchange high-performance liquid chromatography method. More recently, A/I ratios were calculated from the D/L ratios of valine measured with the automated reverse-phase chromatography technique using the equations established by Whitacre et al. (2017). More information on these diverse analytical methods and sample preparation can be found in Hearty and Kaufman (2000, 2009), Hearty (2010) and Kerans et al. (2019).

4. Definition and description of the Whale Point Formation

In the following sections, we formally define the Whale Point Formation as a new unit in the lithostratigraphic record of the Bahamas archipelago.

4.1. Origin of the name

The name of this new formation is derived from that of the apex of a NNW-SSE trending headland in the northern part of Eleuthera Island (toponymy from the topographic map Eleuthera, sheet 3, scale 1:25,000; Bahamas Government, 1969).

4.2. Holostratotype and parastratotype

Both the holostratotype and the parastratotype of the WPF are to be found on Eleuthera Island. The former is situated on the aforementioned Whale Point headland (N25°27′28.94″; W76°37′09.98″), the latter corresponds to a rocky cove called the Boiling Hole or Queen's Bath (N25°25′56.90″; W76°35′51.63″) positioned on the Atlantic coast of North Eleuthera about 3.5 km SE of Whale Point. These sections are scrupulously described as an appendix.

4.3. History

As previously mentioned, this unit was first identified on San Salvador, and named the Almgreen Cay Formation by Hearty and Kindler (1993a). These deposits typically consist of paleosol-capped skeletal eolianites, and were correlated with MIS 5a because of their position (seaward of landforms dated to MIS 5e) and the results of AAR dating. This addition to the Bahamian stratigraphic record known at that time generated much controversy in the subsequent years (Carew and Mylroie, 1994; Hearty and Kindler, 1994; Carew and Mylroie, 1995a and 1995b) mostly because, on San Salvador, stratigraphic relationships are not straightforward. Exposures showing the ACF overlying MIS 5e rocks, but separated from the latter by an intervening paleosol, were later observed at several localities in Eleuthera (Hearty and Kindler, 1995a; Hearty, 1998), but the controversy persisted as several following authors (Carew and Mylroie, 2001; Panuska et al., 2002; Mylroie, 2008) correlated these deposits with the sea-level fall at the end of the LIG. The ACF was informally renamed "Whale Point Formation" by Kindler et al. (2010), and this name was used in several subsequent papers (Godefroid, 2012; Godefroid et al., 2019; Jackson, 2017).

4.4. Description

4.4.1. Geomorphological characteristics

The WPF forms moderate-elevation ridges (up to 15 m high) that are always located on the bank margins, a few 100's of m to up to 2 km landward of the platform edges. Generally, these ridges have been partly eroded during the Holocene transgression, and appear as a series of headlands attached to a main island (e.g., Crab Cay - Almgreen Cay - The Bluff in San Salvador; Fig. 3) or as chains of small islets (e.g., Booby Rocks on Mayaguana Bank; Fig. 4). These outcrops commonly form anchors for subsequent deposits of Holocene and modern age (Figs. 3 and 4).

4.4.2. Sedimentological characteristics

The WPF exposures display many medium- and large-scale cross bedding, the most conspicuous of which are tabular-planar and wedge-planar sets of steeply dipping, cm-thick foresets (Fig. 5). Set thickness cannot always be precisely measured as the foreset bases may be located below sea level. On the average, it varies between 0.5 and more than 5 m. Foresets are slightly convex upward, and usually dip landward with an angle between 30 and 35°. Thick sets of lowangle (10 to 15°) cross-beds and planar beds also occur, particularly on the seaward side and in the upper portions of the WPF ridges (Fig. 5). These sets generally truncate the high-angle cross-beds (Fig. 5). At a smaller scale, mm-thin climbing translatent stratification (CTS) and grainfall lamination, as well as cm-thick sandflow cross-strata (Hunter, 1977; Loucks and Ward, 2001) can also be observed. Notable networks of calcrete-cored rhizoliths (i.e., rhizocretions, Klappa,

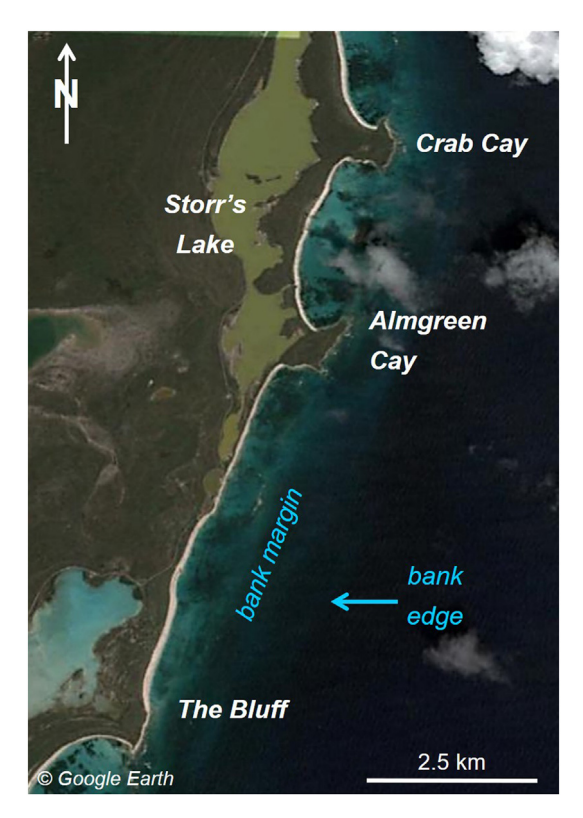


Fig. 3. Satellite image of a portion of the eastern, windward coast of San Salvador Island (see location on Fig. 1) where the WPF forms low-elevation headlands (from North to South: Crab Cay, Almgreen Cay, and The Bluff). The bank edge is located at ca. 1 km seaward of the headlands.

1980) may penetrate the upper part of the WPF down to a depth of 3 m (Fig. 6a). At some exposures, the uppermost sets of the formation comprise m-scale, hollow cylinders up to 30 cm in diameter (i.e, megarhizoliths, Alonso-Zarza et al., 2008; Fig. 6b) that locally protrude at the surface.

4.4.3. Lithological characteristics

The WPF consists of laminated, medium- to coarse-grained, friable, yellowish bioclastic calcarenites. Diagnostic pink fragments of the encrusting foraminifer $Homotrema\ rubrum$ (Fig. 7b) can frequently be observed with a hand lens. These calcarenites are best described as loosely packed skeletal grainstones. The percentage of bioclasts is high (79.8%; n=20; Kindler and Hearty, 1996). Benthic and encrusting

foraminifers, red and green algae (e.g., *Halimeda* sp.), corals, echinoids, and mollusks (bivalves and gastropods) represent the most common biogenic fragments (Fig. 7a). Soritidae (e.g., *Archaias* aff. *angulatus*, Fig. 7c) and Miliolidae (e.g., *Quinqueloculina* sp., *Triloculina* aff. *quadrilateralis*, *Triloculina* aff. *rotunda*; *Pyrgo* sp., Fig. 7d) are the main families of benthic foraminifers observed in the WPF. Amphisteginidae (e.g., *Amphistegina* aff. *lessonii*) and Textulariidae (e.g., *Textularia* aff. *candeiana*) occur in a few samples, whereas planktonic foraminifers have never been observed. Ooids, oolite lithoclasts and peloids may be found near the base of the formation at some sites.

WPF rocks exclusively contain aragonite, high- and low-Mg calcite (LMC). Considering the nature of constituent particles and the amount of cement, the percentage of LMC can be estimated between 5 and 10%, and that of metastable carbonate minerals between 90 and 95%. Allochems are usually well preserved, but some grain leaching and micritization may be observed in a few samples. Cement percentage is very low (between 0 and 8.6%; n = 20; Kindler and Hearty, 1996). Cement is generally composed of small (<20 μ m) crystals of LMC forming menisci (Fig. 7a) and dripstones between and beneath grains, respectively. Microcrystalline "grain-skin cement" (Land et al., 1967) may also be present in some samples. WPF rocks are very porous. Predominant porosities are of intergranular (close to 40%; Kindler and Hearty, 1996) and intragranular type. Sparse micromoldic porosity may also occur in some samples.

4.4.4. Geochemical characteristics

Whole-rock AAR data obtained from the WPF samples (n=35) are reported in Table 2. The average of alloisoleucine/isoleucine (A/I) values from the retained samples (n=33) is 0.301 ± 0.042 . As demonstrated in previous studies for this and other Bahamian units (Hearty and Kaufman, 2000, 2009), there is a gradual increase in A/I values from the northern islands (e.g., Abaco, A/I = 0.280) to the southern reaches of the archipelago (e.g., Long, average A/I = 0.317).

Beier (1987) obtained the following geochemical data from WPF calcarenites (n = 4) collected at The Bluff (San Salvador): Al and Fe occur in extremely low concentrations; MgO = 2.5 to 3.0 wt%; Sr = 3000 ppm; $\delta^{13}\text{C} = +2$ per mil; $\delta^{18}\text{O} = -2$ per mil; TOC = 0.1%. Similar isotopic values were more recently obtained from exposures in Eleuthera and Long Island (L. Vimpere, pers. comm. 2021).

4.5. Facies variations

At several sites (e.g., The Bluff, San Salvador, Fig. 8a), the WPF encompasses a thin, subhorizontal layer devoid of physical sedimentary structures that commonly includes cm-sized calcitic nodules, rhizocretions and numerous shells of the terrestrial gastropod *Cerion* sp. (Fig. 8b). The petrographic composition of this layer is identical to that of the rest of the WPF. However, grain leaching and needle-fiber



Fig. 4. Oblique aerial photograph of Booby Rocks near the NW corner of Mayaguana Bank, about 2 km NNE of the island shoreline (location on Fig. 1). These small (150 × 70 m) cays are the exposed remnants of a NW-SE trending, mostly submerged WPF ridge which supports a modern coral reef. Yellow arrow points to the cliff face illustrated in Fig. 5. Photo by P. Kindler.



Fig. 5. Partial view of the southern side of the largest cay at Booby Rocks (see location on Fig. 4). Cliff face shows a 4 m-thick set of large-scale foresets (f) overlain by a 3.5 m-thick set of lowangle cross beds (t). White arrow points to truncation surface between foresets and topsets. Cliff elevation varies between 10 and 12 m. Visible portion of the cliff is about 40 m long. Note that foreset beds do not dip landward (i.e., towards the island), but to the West (35/270).

calcite cement are more common in the former than in the latter. According to Beier (1987), the Al and Fe concentrations are slightly higher in this deposit than in the cross-bedded strata; MgO = 1.5 wt%; Sr = 3000 ppm; δ^{13} C = -3 per mil; δ^{18} O = -4 per mil; TOC = 0.1%.

4.6. Macrofossil content

Shells of *Cerion* sp. are the only macrofossils found in the WPF. These shells essentially occur in the thin layers devoid of physical sedimentary structures described in the previous section. According to Hearty et al. (1993), WPF *Cerion* group from San Salvador is characterized by a large shell and limited axial ribbing. However, a more recent study (Hearty and Schellenberg, 2008) shows that *Cerion* sp. found in the WPF are highly variable in size, shape, colour and ornamentation. Moreover, efforts to identify this land snail specifically have been hampered by the lack of consensus with respect to species-level taxonomy (Hearty and Schellenberg, 2008).

4.7. Boundaries

4.7.1. Upper boundary

The upper limit the WPF is always sharp, and usually corresponds to the lithosphere - atmosphere boundary (Fig. 6a). At some localities, however, the formation is overlain by sub-recent sands (Fig. 9a) or by the Rice Bay Formation (Holocene). In all cases, the upper reaches of the WPF reveal a complex *terra-rossa* paleosol comprising laminated micritic crusts, breccia horizons and rhizocretions (Figs. 6a and 9a).

4.7.2. Lower boundary

The basal limit of the WPF is rarely visible as it is generally located below sea level. Where exposed, it separates the WPF from the underlying Grotto Beach Formation that has been dated to MIS 5e (Chen et al., 1991; Thompson et al., 2011). The lower boundary of the WPF is sharp. The formation overlies either a carbonate paleosol developed at



Fig. 6. A: Upper portion of the WPF at Crab Cay, San Salvador, displaying an impressive network of rhizocretions underlying a cm-thick laminated micritic crust, indicated by a white arrow, and a breccia-rich paleosol. Geological hammer for scale is 36 cm long. B: Megarhizoliths (not to be mistaken for fossil tree trunks) in the upper part of the WPF at Cape Verde, southern tip of Long Island. Hammer is 35 cm long.

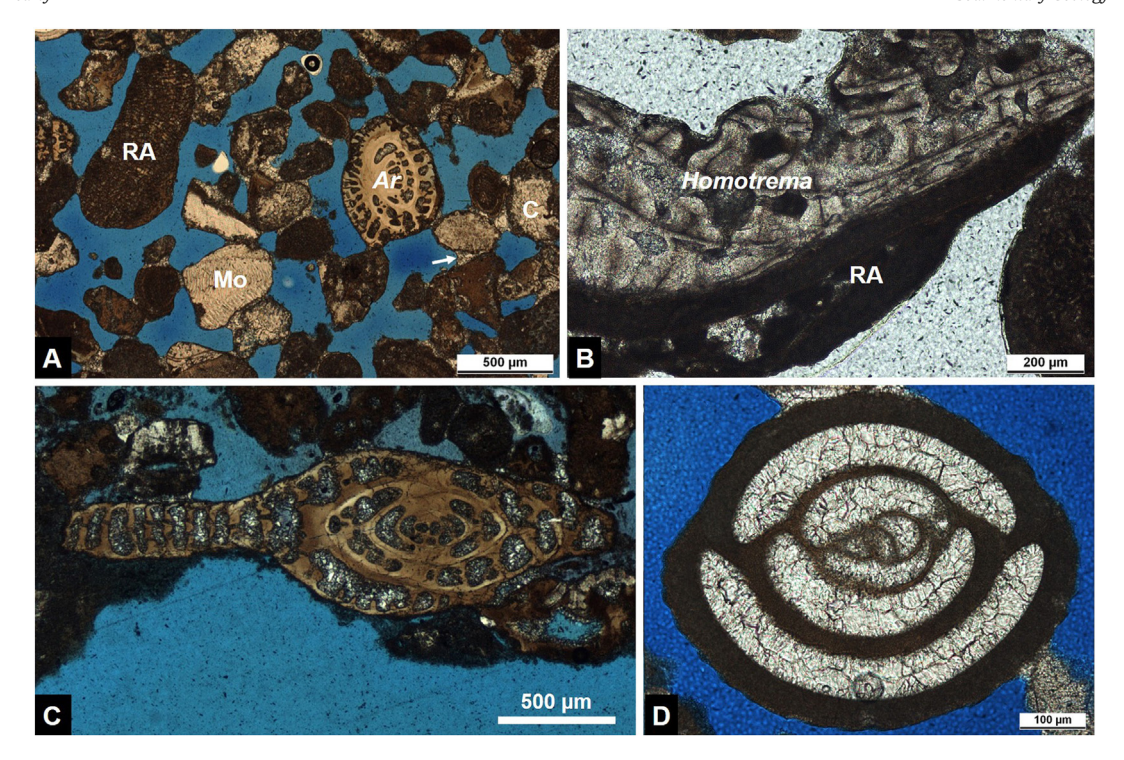


Fig. 7. A: Microfacies of the WPF. Note abundance of bioclasts (RA = red algae; Ar = *Archaias* sp.; C = coral; Mo = mollusk), high intergranular porosity (blue areas), scarce sparry cement forming menisci at grain contacts (white arrow); sample MB 32, Whale Point, Eleuthera. B: *Homotrema rubrum* encrusted on red-algal fragment (RA); sample SS 110, Man Head Cay, San Salvador. C: *Archaias* aff. *angulatus*; sample SS 141, Green Cay, San Salvador. D: *Pyrgo* sp.; sample EL 208, Rainbow Cay, Eleuthera.

the top of the Grotto Beach Formation (Fig. 9b; Nawratil de Bono, 2008), or a karstic surface carved into the latter unit (Fig. 9c and d). Between 5 and 40 cm thick, the paleosol includes a basal micritic crust overlain by a breccia layer (Ck horizon). The breccia blocks show a fitted fabric (Fig. 9b), and consist of oolitic grainstone separated and overlain by a pink, friable, sandy matrix (B horizon) comprising a pedogenized mix of bioclasts and ooids. Predominant minerals are calcite and aragonite; the clay content of this matrix amounts to less than 5% (Brentini, 2008; Nawratil de Bono, 2008).

4.8. Dimensions and geographic extent of the WPF

WPF exposures have been identified on Abaco, Grand Bahama, Gun Cay (Bimini Islands), New Providence, Eleuthera, Cat, Long, San Salvador, Rum Cay and the Exuma Chain (Fig. 1). The formation appears to be missing from Andros and, except for Mayaguana (Godefroid, 2012), from the islands forming the southern part of the Bahamian archipelago (Crooked, Acklins, Great Inagua) as well as from those standing on the Caicos platform (e.g., West Caicos; Kerans et al., 2019). The WPF has thus a wide horizontal extent (more than 600 km), but exposures are discontinuous and the visible thickness of the formation does not generally exceed 15 m.

5. Discussion

5.1. Age of the Whale Point Formation

Several attempts have been made to use paleontological criteria (i.e., *Cerion* sp. snails) for establishing the stratigraphy of the Bahamas islands (e.g., Garrett and Gould, 1984). However, these efforts have been mostly unsuccessful because of the very large number (ca. 600) of *Cerion* species (http://invertebrates.si.edu/cerion), and the influence of geographical and ecological factors on the snail morphology (Rose, 1983; Carew and Mylroie, 1995a; Gould, 1997; Hearty, 2010). As

demonstrated among pre-Columbian to historical populations of *Cerion* sp. highly mixed by human agencies, there is prolific hybridization locally and among islands. These features suggest that anagenesis (morphological change) rather than cladogenesis (speciation) is the determinate process in shell morphology, thus bringing into question the accuracy of the actual taxonomic identification.

Nonetheless, its stratigraphic position between a discontinuity (paleosol or karstic surface) developed at the top of rock bodies radiometrically dated to the LIG (Fig. 9c) and a glacial paleosol capped by Holocene deposits (Fig. 9a) undoubtedly indicates that the WPF was formed after MIS 5e, but before the deposition of the earliest Holocene sediments, i.e., between ca. 118 and 7 ka BP. As sedimentation only takes place on Bahamian banks when they are fully or partially submerged, the deposition of the WPF must have occurred during one of the two major sea-level events that characterize the abovementioned time interval: the MIS 5c (ca. 100 ka BP) or the MIS 5a (ca. 80 ka BP) high stands. Finally, margins of error considered, 27 out of the 35 obtained whole-rock A/I ratios (i.e., 77%; Table 2) correspond to aminozone C (0.25 < A/I < 0.35), which is correlated to MIS 5a (Hearty and Kaufman, 2000, 2009). When excluding the samples from Mayaguana, that likely experienced a different temperature history due to the nature of the exposure (Fig. 4), this percentage increases to 86%. The AAR geochronology might not be as renowned as the U—Th and ¹⁴C dating methods, but it has proven to be invaluable for assessing ages to rock units than cannot be dated with the latter techniques (e.g., Harmon et al., 1983; Hearty et al., 1992; Hearty and Kaufman, 2000, 2009; Murray-Wallace et al., 2016).

5.2. Genesis of the Whale Point Formation

All skeletal grains comprising the WPF are of marine origin. However, the displayed physical sedimentary structures (e.g., large-scale cross bedding, Fig. 5; CTS) collectively and unambiguously identify this unit as a wind-deposited sand body. That the WPF was formed in

Table 2 Amino-acid racemization data obtained from the Whale Point Formation, A/I = alloisoleucine/isoleucine

Lab #	Field #	Exposure	Island	GPS coordinates		A/I		Ref
1668A	AGF-1a	Great Guana Cay	Abaco	N26°39′29″	W77°05′26″	0.280	±0.019	1
1464A	EFI1e	First Bay	Eleuthera	N25°24′34″	W76°33′17″	0.299	± 0.002	2
1466A	EKS1a	Kemps Pond	Eleuthera	N25°07′07"	W76°06′56″	0.300	± 0.001	2
1467B	ERC2c	Rainbow Cay	Eleuthera	N25°20′04″	W76°25′13″	0.248	± 0.003	2
1562A	EBH1g	Boiling Hole	Eleuthera	N25°25′56″	W76°35′51″	0.302	± 0.003	2
1573A	EWP2k	Whale Point	Eleuthera	N25°27′28″	W76°37′09″	0.309	± 0.001	2
			Average			0.292	± 0.025	
1686A	NGC-1a	Green Cay	New Providence	N25°06′23″	W77°11′30″	0.275	± 0.019	3
1687A	NGC-2b	Green Cay	New Providence	N25°06′23″	W77°11′30″	0.279	± 0.010	3
1469A	NGC2d	Green Cay	New Providence	N25°06′23″	W77°11′30″	0.378	± 0.004	3
		J	Average			0.311	± 0.058	
0021B	TB1c	The Bluff	San Salvador	N23°59′42″	W74°27′30″	0.333	± 0.002	4
0022B	AC1c	Almgreen Cay	San Salvador	N24°02′17"	W74°26′16″	0.312	± 0.001	4
0021A	TB1a	The Bluff	San Salvador	N23°59′42″	W74°27′30″	0.283	± 0.003	4
0022A	AC2a	Almgreen Cay	San Salvador	N24°02′17″	W74°26′16″	0.284	± 0.003	4
8722	SS160	Crab Cay	San Salvador	N24°03′49″	W 74°25′46″	0.289	± 0.014	0
8723	SS141	Green Cay	San Salvador	N24°08′20″	W74°30′35″	0.334	±0.016	0
		,	Average			0.306	±0.034	
7197 A	Fab212	Port Boyd	Rum Cay	N23°42′34″	W74°49′14″	0.385	± 0.006	0
1787A	XHC-1a	Hawksbill Cay	Exumas	N24°30′12″	W76°45′35″	0.376	± 0.002	5
1470A	XS1ab	Stocking Island	Exumas	N23°31′59″	W75°45′58″	0.307	± 0.003	5
	ST8	Stocking Island	Exumas	N23°31′59″	W75°45′58″	0.295	±0.005	6
	ME19	Stocking Island	Exumas	N23°31′59″	W75°45′58″	0.294	± 0.004	6
			Average			0.318	±0.039	
1477A	LCC1a	Clarence Town	Long	N23°06′11″	W74°57′51″	0.306	± 0.009	7
1478A	LBU1a	Bonnie Cord	Long	N23°06′19″	W74°59′02″	0.329	± 0.008	7
	LDB1	Dean's Blue Hole	Long	N23°06′23″	W75°00′31″	0.308	± 0.000	7
	LDB2	Dean's Blue Hole	Long	N23°06′23″	W75°00′31″	0.323	±0.007	7
10,978	LI8	Clem Cay	Long	N23°05′46″	W74°56′24″	0.278	± 0.028	0
10,974	LI24	Buckley	Long	N23°09′35″	W75°04′14″	0.242	± 0.021	0
10,980	LI16	Southern Point	Long	N22°51′09″	W74°51′25″	0.329	± 0.036	0
10,977	LI33	Little Harbour	Long	N22°58′19″	W74°51′10″	0.399	± 0.006	0
13,690	LV4	Dean's Blue Hole	Long	N23°06′23″	W75°00′31″	0.342	± 0.026	8
13,692	LV11	Bonnie Cord	Long	N23°06′19″	W74°59′06″	0.213	± 0.021	8
13,692	LV12	Bonnie Cord	Long	N23°06′19″	W74°59′00″	0.246	± 0.006	8
13,700	LI47	Buckley	Long	N23°09′35″	W75°04′14″	0.253	± 0.008	0
13,701	LI52	Buckley	Long	N23°09′35″	W75°04′14″	0.258	± 0.012	0
13,702	LI53	Little Harbour	Long	N22°58′17″	W74°50′51″	0.285	± 0.007	0
13,703	LI61	Little Harbour	Long	N22°58′19″	W74°51′10″	0.333	± 0.007	0
13,705	LI65	Roses E coast	Long	N23°01′12″	W74°52′22″	0.246	± 0.007	0
,			Average			0.293	±0.048	-
			Average*			0.317	±0.011	
8710	Fab116	Booby Rocks	Mayaguana	N22°27′57″	W73°06′33″	0.485	±0.056	9
16,993	Fab117	Booby Rocks	Mayaguana	N22°27'57"	W73°06′33″	0.470	± 0.001	0
16,994	Fab120	Booby Rocks	Mayaguana	N22°27'57"	W73°06′33″	0.442	± 0.035	0
10,001	140120	Doody Rocks	Average	1122 21 31	1113 00 33	0.466	±0.035	Ü

measured A/I values (IE HPLC); A/I values calculated from D/L Val (RPC).

Ref.: original AAR data found in the following papers:

- 0: Kindler unpublished data
- 1: Hearty and Kaufman (2000)
- 2 : Hearty (1998)
- 3: Hearty and Kindler (1997)
- 4: Hearty and Kindler (1993a, 1993b)
- 5 : Hearty unpublished data
- 6: Mazzolini (2000)
- 7 : Hearty (2010)
- 8 : Vimpere (2017) 9 : Godefroid (2012)
- a subaerial setting is further confirmed by the presence of terrestrial gastropods and the widespread occurrence of rhizocretions (Fig. 6). The original morphology of the WPF has been considerably altered by coastal erosion and karst denudation since MIS 5a. Satellite imagery and field mapping nevertheless show that it comprised moderate-elevation (15 to 20 m) transverse dunes (e.g., along the eastern coast of San Salvador, Fig. 3), that can be interpreted as precipitation ridges (Hesp et al., 2005), and narrow dune fields supporting low-elevation "haystack" landforms (e.g., Whale Point Boiling Hole area; see appendix). The predominance of large-scale, steeply dipping foresets and their position above a paleosol, both indicate that the WPF eolianites are fos-

sil "transgressive" (Hesp et al., 2005) or "advancing" (Mauz et al., 2013;

Rowe and Bristow, 2015a and 2015b) dunes, i.e., dunes that encroached inland, and were decoupled from their source beaches. The occurrence of truncated large-scale foresets overlain by low-angle cross-beds (Fig. 5) has been observed elsewhere (Rowe and Bristow, 2015a and 2015b), and interpreted as representing dune advance (foresets), stoss-slope erosion (truncation surface), and dune accretion (low-angle cross-beds). Modern advancing dunes are few in the Bahamas, but some have been observed by the senior author in the dryer southeastern portion of the archipelago (Fig. 10). Cement geometries and crystal size indicate that early diagenesis took place in the meteoric vadose environment. The high proportion of unstable minerals still present in the WPF further suggests that the formation was subsequently

^{*} average excluding RPC values.

Fig. 8. A: Coastal outcrop at The Bluff, San Salvador, revealing the facies variations within the WPF. Note thick alteration profile at the top of the exposure. Yellow arrow points to protruding structureless interval illustrated in panel b. Person for scale is 1.84 m tall. B: Close-up view of the layer devoid of sedimentary structures including calcitic nodules and *Cerion* sp. snails. Hammer handle is 2 cm wide.

protected by an aquiclude (i.e., the overlying calcrete; Ward, 1973, 1997). The fairly elevated Sr concentration confirms the presence of pristine aragonitic bioclasts within the host rock, whereas the δ^{13} C and the δ^{18} O values reflect the marine origin of the allochems and the influence of fresh-water diagenesis, respectively.

The dm-thick layers devoid of physical sedimentary structures interspersed in the WPF (Fig. 8a) have been caused by pedogenic alteration as indicated by the occurrence of rhizocretions, calcitic nodules and abundant shells of *Cerion* (Fig. 8b). These layers have been designated as "pisolitic paleosols" (Brown, 1984), "immature caliche profiles" (Beier, 1987) or "protosols" (Hearty and Kindler, 1993a). The slight increase in Al and Fe content, the decrease in MgO concentration and

the more depleted isotopic values (Beier, 1987), all signify that these layers have been exposed to the input of atmospheric dust and to fresh-water diagenetic processes for a longer time than the eolian sands of the WPF.

5.3. Correlations

The WPF can confidently be correlated with the Mujeres Eolianite exposed in the NE part of the Yucatan Peninsula (Mexico; Ward, 1973, 1975, 1997; Kelley et al., 2011). This unit displays geomorphological, sedimentological and petrographic characteristics that are analogous to those of the WPF, and further occurs in a comparable setting and

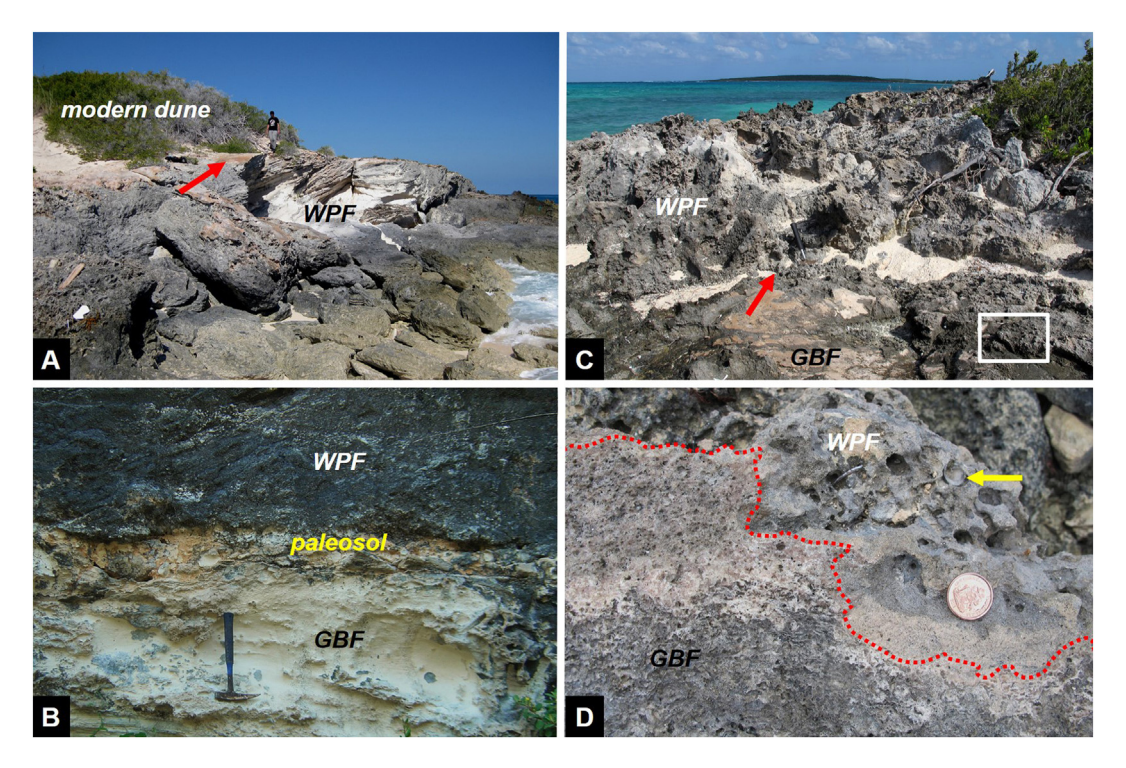


Fig. 9. A: Partial view of a sea cliff at First Bay, Eleuthera (for details, see Hearty, 1998), showing the upper boundary of the WPF overlain by a vegetated dune of recent age. The boundary is marked by a thin micritic crust (red arrow) capping a paleosol. Person for scale is 1.85 m tall. B: Partial view of the Rainbow Cay roadcut, Eleuthera (Hearty, 1998; Brentini, 2008), showing the lower boundary of the WPF. As at the type section, the boundary consists of a breccia-rich carbonate paleosol developed at the expense of the underlying Grotto Beach Formation (GBF). The latter consists of an oolitic eolianite at this location. Hammer for scale is 36 cm long. C: Partial view of the Little Harbour exposure, Long Island, showing the superimposition of the Whale Point and Grotto Beach formations, the latter being represented by a coralgal reef. Red arrow points to the karstic surface between the two units. White rectangle shows the position of panel d. Geological hammer for scale is 30 cm long. D: Close-up view of the lower boundary of the WPF at the same exposure. Note corrugated aspect typical of karstic processes. Yellow arrow points to a *Cerion* sp. shell in the WPF. Coin for scale is 2 cm in diameter.



Fig. 10. Possible modern analogues of the WPF eolianites. A: Recent advancing dune along the north shore of Mayaguana near Curtis Creek (N22°24′17.64″N; W72°55′20.83″). The ridge is unlithified, poorly vegetated, and about 4 m high. It overlies reefal limestone of Early Pleistocene age and is not connected to a beach. B: Closer view of the boundary between the recent dune and the coralgal limestone. Note large partly eroded coral head in the foreground. Hammer for scale is 36 cm long. C: Similar view as panel a from Timber Bay, Mayaguana (N22°20′ 14.81″; W72°43′51.74″). There, the recent dune overlies a dolomitized coralgal framestone of Gelasian age. Person for scale is 1.58 m tall.

morphostratigraphic position. The Mujeres Eolianite has not been dated yet, but it is considered as the youngest Pleistocene dune ridge of that area, and thought to have been deposited during the regressive phase of MIS 5e, MIS 5c or MIS 5a (Ward, 1997).

The WPF can be largely related to the Southampton Formation (SF) outcropping in Bermuda (Land et al., 1967; Vacher and Hearty, 1989; Vacher et al., 1995; Vacher and Rowe, 1997; Hearty, 2002). This unit is however far more complex than the WPF. The SF comprises one main eolian body which includes several protosols and forms ridges up to 60 m high. This prominent eolianite is onlapped downdip by coarse-grained, coral and shell-rich marine deposits exposed at around 1 m above sea level, and overlain by a 10 m-high regressive eolianite. The eolian facies of the SF are very similar to that of the WPF, although constituent grains are in general more rounded in the former than in the latter. By contrast, equivalent marine facies are missing in the WPF, which is likely related to glacio-hydroisostatic processes (Potter and Lambeck, 2003; Wainer et al., 2017; see Section 5.6.). The main part of the SF has been assigned to MIS 5c and/or MIS 5a on the basis of AAR data (Harmon et al., 1983; Hearty et al., 1992), and the overlying marine and eolian sediments to the late portion of MIS 5a based on both AAR measurements (Vacher and Hearty, 1989; Hearty et al., 1992) and a number of U-Th dates on Oculina coral fragments (Harmon et al., 1983; Ludwig et al., 1996; Muhs et al., 2002, 2020). These geochronological data are consistent with those obtained from the WPF.

By contrast, except for the correspondence in age, the WPF markedly differs from the MIS 5a record on Grand Cayman. Indeed, Unit F of the Ironshore Formation consists of cross-bedded oolitic grainstones deposited under marine conditions and exposed up to +5 m above sea level (Coyne et al., 2007). This discrepancy has yet to be further investigated, but it might be related to the method applied to date this unit (U-series dating on mollusk shells).

5.4. Significance of the WPF for Bahamian stratigraphy

As mentioned in Section 4.3., our addition of the WPF (previously ACF) to the stratigraphic record of the Bahamas islands in the early 1990's (Hearty and Kindler, 1993a and 1993b) was denied at that time, because the definition of this unit was perceived as solely based

on morphological criteria and AAR data (Carew and Mylroie, 1995a, 1997, 2001). The formal description of the WPF presented in this paper hopefully closes this debate. The WPF comprises distinctive depositional phases, defined by numerous criteria, that occurred during MIS 5a. These eolianites do not represent a lowering of sea level at the end of MIS 5e (Carew and Mylroie, 1995a, 1997, 2001), and thus must not be assigned to the Grotto Beach Formation. That said, eolian and foreshore deposits accumulated during the late MIS 5e regression are common across the Bahamas (e.g., Gerhardt, 1983; White and Curran, 1995; Godefroid, 2012; Kerans et al., 2019). However, they are mostly composed of ooids and peloids (Kindler and Hearty, 1996; Kerans et al., 2019), and are generally superposed or off-lapping older MIS 5e rock bodies. The nearly pure skeletal composition of the WPF deposits characterizes another sedimentation phase that clearly differs from those of MIS 5e.

5.5. Constraints on the elevation of relative sea level in the Bahamas during MIS 5a

The highest elevation of relative sea level (RSL) in the Bahamas during MIS 5a has long been a matter of controversy. The results of U—Th dating performed on submerged speleothems from Grand Bahama (Li et al., 1989; Lundberg and Ford, 1994) and Andros (Richards et al., 1994) show that peak RSL reached no higher than 18 to 15 m below present at that time, which agrees with estimates relying on uplifted-coral (e.g., Potter et al., 2004) and oxygen-isotope (Waelbroeck et al., 2002; Spratt and Lisiecki, 2016) data. By contrast, assuming that the WPF (then ACF) eolianites were tied to their source beaches, Hearty and Kindler (1993a, 1995b) and Hearty and Kaufman (2000) proposed that RSL was within 0 to -5 m of the modern datum during the formation of this unit. Our recognition of these landforms as advancing dunes justifies to reconsider this assessment.

The elevation of RSL in the Bahamas during MIS 5a, can be roughly estimated from the constituent particles of the WPF. The lack of planktonic foraminifers and the scarcity of robust amphisteginidae among bioclasts preclude to place the locus of formation of these grains on a submerged forereef terrace near the platform edge (Hallock and Glenn, 1986), as should have been the case if sea level had been at ca. 15 to 18 m below the present one (Li et al., 1989; Lundberg and Ford,

1994; Richards et al., 1994). The repeated occurrence of Homotrema rubrum fragments in the WPF eolianites indicates a certain proximity to reefal areas (Rose and Lidz, 1977; Gischler and Möder, 2009). Furthermore, the presence of numerous debris of soritidae and miliolidae suggests the existence of water bodies landward of the reefs because these foraminifers thrive in quiet and shallow, seagrass-floored, lagoonal areas (Rose and Lidz, 1977; Li and Jones, 1997). Thus, the constitutive bioclasts of the WPF were probably formed in narrow lagoons behind platform-margin reefs. The petrographic composition of the WPF is further characterized by the lack of ooids, excepting those reworked from the underlying or laterally juxtaposed Grotto Beach Formation. Bahamian-type ooids form in well-agitated, warm, and shallow waters supersaturated in CaCO₃ (Bathurst, 1975; Rankey and Reeder, 2011; James and Jones, 2015; Harris et al., 2019). The occurrence of hermatypic coral fragments in the WPF shows that bank waters must have been sufficiently warm and supersaturated in CaCO₃ at that time to trigger the precipitation of ooids. The absence of these particles in the WPF is thus likely related to unfavorable hydrodynamic conditions. Indeed, the water layer on the platforms must be suitably deep to generate vigorous tidal currents conducive to ooid formation (Hine, 1977; Harris et al., 2019). The first pulse of oolitic production in the Holocene has been dated at ca. 6.8 ka BP (Hearty and Kaufman, 2009). These grains are now found in the North Point Member (Carew and Mylroie, 1985; Kindler and Hearty, 1996), an eolianite of middle Holocene age deposited when sea level was between 6 and 7 m below the present datum, and flooding of the Bahamian banks was ca. 50% of what it is presently (Boardman et al., 1989). The absence of ooids in the WPF eolianites thus provides an upper limit for the elevation of the coeval sea level at around 7 m below the modern stand. If sea level had been higher (i.e., between 0 and -5 m below present; Hearty and Kaufman, 2000), ooids would have been produced. A lower limit is given by the depth of the platform edge (≥20 m; Bergman et al., 2010), but as discussed above, the faunal content of the WPF indicates a lagoonal source for the sediments, implying that MIS 5a sea level could not have been that low. Thus, we conclude that sea level was probably between 7 and 11 m below the present datum during the formation of the constituent grains of the WPF. This estimate is consistent with the reconstruction of Toscano and Lundberg (1999) who, based on submerged in-situ corals from the South Florida margin, estimated the peak RSL during MIS 5a at -9 m.

Determining the elevation of global mean sea level (GMSL) from RSL markers is an increasingly arduous task because the position of the latter depends not only on eustacy and regional tectonics, but also on isostatic uplift due to karstic denudation (Opdyke et al., 1984; Mylroie et al., 2020), glacio-hydro-isostatic processes (i.e., glacial isostatic adjustment, GIA; Dutton and Lambeck, 2012; Dutton et al., 2015, and references therein), and dynamic topography (Dutton et al., 2015; Austermann et al., 2017). Considering the tectonic setting of the Bahamas and the short time span elapsed since the formation of the WPF, most of these factors can be put aside with the exception of GIA. However, recent GIA modelling using a low-viscosity upper mantle in analyzing data on the Pacific coast relative to the Atlantic region, and excluding the Bahamian speleothem (Richards et al., 1994) and eolianite (Hearty and Kaufman, 2000) data from the analysis, constrained peak GMSL at 8.5 \pm 4.6 m below present datum during MIS 5a (Creveling et al., 2017). The RSL elevation obtained from our examination of the WPF (7 to 11 m below present) can thus be considered as a fairly accurate estimate of MIS 5a GMSL. Such an agreement between the elevation of RSL markers in the Bahamas and GIA-modeled sea level was also recognized by Muhs et al. (2020) for the LIG. However, this estimation challenges the opinion of Dorale et al. (2010) who, based on speleothem evidence from Mallorca, reckoned that MIS 5a was at least as ice-free as the present. However, considering that Mallorca is located closer to the position of the former northern hemisphere ice sheets than the Bahamas, it would actually be surprising that the RSL records from both regions would perfectly match.

5.6. Sea-level and climate fluctuations in the Bahamas during MIS 5a

Previous investigations have demonstrated that both sea level and climate varied significantly and abruptly between 90 and 70 ka BP. Using different approaches, Siddall et al. (2003) and Potter et al. (2004) identified two highstands of sea level, separated by a short regression, centered at ca. 84 and ca. 77 ka BP, respectively (Fig. 11). Furthermore, sudden shifts in the amount of rainfall caused by displacements in the mean annual position of ITCZ have been inferred from the examination of basinal sediments of MIS 5 age from the Caribbean region (Peterson et al., 2000; Gibson and Peterson, 2014; Zhuravleva and Bauch, 2018). These changes have been linked to large millennial-scale temperature oscillations over the North Atlantic (Dansgaard et al., 1993; North Greenland Ice Core Project, 2004; Rasmussen et al., 2014). The facies pattern observed on several WPF exposures can be interpreted as a record of these instabilities in a coastal setting.

At many locations (e.g., The Bluff in San Salvador, Fig. 8a; Booby Rocks on the Mayaguana Bank; Port Boyd in Rum Cay), the WPF encompasses two cross-bedded eolian rock bodies separated by one thin, structureless protosol. In other words, the WPF records two phases of eolian deposition, logically following episodes of sediment production, separated by one interval of negative sediment budget and pedogenesis. In the Bahamas, shallow-water carbonate production can only take place when the banks are at least marginally flooded, i.e., when sea level is fairly close to modern datum. Moreover, unlike seawardprograding eolianites (e.g., Holocene biopelsparite II, Davaud and Strasser, 1984; Hanna Bay Member, Carew and Mylroie, 1985), deposition of advancing dunes essentially occurs during the onset of regressions (Rowe and Bristow, 2015b) and preferentially in dry and windy climatic conditions that prevent dune stabilization by vegetation. Finally, soils mostly form during warm and humid intervals characterized by reduced wind activity that favors the development of vegetation, and limits sand transport.

Based on these premises, the depositional history of the WPF can be summarized as follows (Fig. 11). The production of the WPF

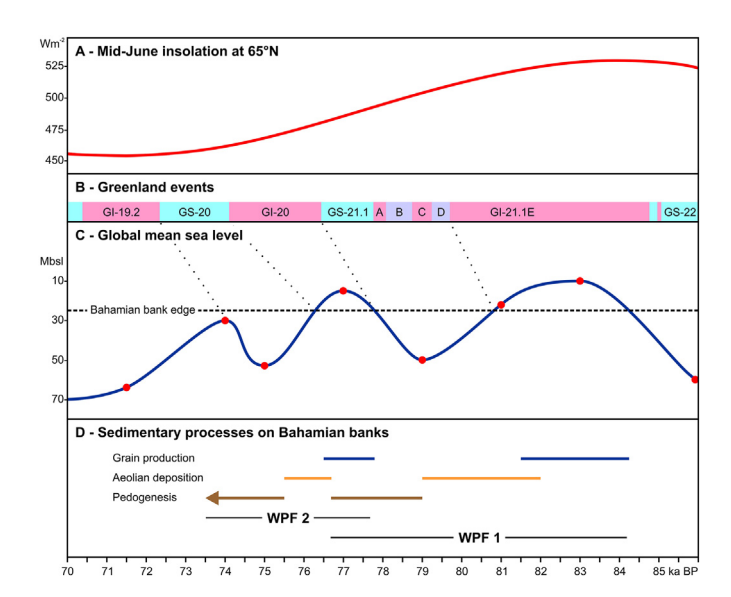


Fig. 11. A: Mid-June insolation curve at 65°N for the time interval between 86 and 70 ka BP (after Berger, 1978). B: Chronology of Greenland events (after Rasmussen et al., 2014). GI = Greenland Interstadial; GS = Greenland Stadials. C: Global mean sea level derived from the data points (red dots) of Siddall et al. (2003). According to these authors, peak GMSL during MIS 5a (at 84 ka BP) was 30 m below present datum. We equated this data point to the maximum sea level elevation during MIS 5a estimated from our study (i.e., -9 ± 2 m) and obtained the other points by adding 21 m to Siddall et al.'s data. Note that these high-frequency sea-level changes are not recorded in the insolation curve (panel a). Mbsl = meters below sea level. D: Reconstruction of the sedimentary events on the Bahamian banks during MIS 5a. WPF1/2 = lower/upper eolianite of the WPF.

sediments logically began during the first MIS 5a highstand when coralgal reef flourished on the flooded bank margins of the Bahamas. An early phase of dune formation took place when the sea receded from the platforms after this first flooding event. An immature soil then developed on these eolian sands during an interval of non-deposition spanning the ensuing highstand while sediment production resumed on the platform margins. A second pulse of dune building occurred during the late MIS 5a regression. Both episodes of eolian sedimentation must have been short because the dunes did not migrate very far bankwards. The early diagenetic microcrystalline LMC cements observed in the WPF eolianites further indicate that these episodes likely occurred under dry conditions characterized by sparse rainfall followed by intense evapotranspiration (Ward, 1973, 1997).

Determining the exact timing of these depositional phases is difficult because the chronologies derived from deep-sea sediments and Greenland ice cores do not fully match (Fig. 11). Based on the sea-level estimates of Siddall et al. (2003), the first phase of eolian deposition could have occurred between ca. 82 and 79 ka BP (mid-MIS 5a regression) and the second phase after ca. 77 ka BP (onset of the late MIS 5a regression). Relying on ice-core records (Rasmussen et al., 2014), these two phases of dune formation could have happened between ca. 79.8 and 76.4 ka BP (cold intervals at the end of Greenland Interstadial 21.1 and Greenland Stadial 21.1) and ca. 74.1 and 72.3 ka BP (GS-20), respectively. This age discrepancy could be related to the difference in applied geochronological methods (isotope stratigraphy versus ice-flow model) and/or to the fact that the structure and timing of millennial-scale variability in some regions appear to have been different from those in the North Atlantic (Rasmussen et al., 2014).

6. Conclusion

The Whale Point Formation, formally defined here, is a new addition to the stratigraphic record of the Bahamas islands. It comprises a series of bioclastic eolianites and protosols exposed on high-energy bank margins throughout the Bahamas archipelago. Its stratigraphic position above deposits dated to MIS 5e and below Holocene sediments constrains its age to the latest Pleistocene, most probably to MIS 5a (ca. 80 ka BP). This age is further corroborated by AAR data calibrated with U—Th ages. Based on their sedimentological characteristics, the WPF eolianites are interpreted as advancing dunes decoupled from their source beaches. Relying on the faunal content, the elevation of RSL during the production of the WPF constituent grains can be assessed at ca. 9 \pm 2 m below the present datum which is consistent with GMSL estimates derived from GIA modelling, suggesting that the Bahamas region might be fairly neutral with respect to surface deformation related to ice-sheet loading.

The WPF further comprises two episodes of eolian sedimentation separated by an interval of negative sediment budget and pedogenesis. These facies changes possibly record millennial-scale sea-level and climate instability during MIS 5a, the latter being likely related to shifts in the mean annual position of the ITCZ and associated rainfall belt in response to changes in the strength of the Atlantic Meridional Overturning Circulation. Thus, the coastal record of the WPF appears to confirm the findings of previous studies based on Greenland ice and basinal sediments that suborbital-period climate fluctuations can occur also during times of reduced ice-sheet extent. Such a possibility must be kept in mind in the context of the present-day, human-induced global warming.

Declaration of competing interest

Neither Pascal Kindler or Paul J. Hearty have any financial or personal relationship with other people or organizations that could inappropriately influence our work.

Acknowledgments

PK's research in the Bahamas was largely supported by several grants offered by the University of Geneva, the State of Geneva, and the Swiss National Science Foundation between 1989 and 2017. Both authors are obliged to many colleagues and students for their help in the field and fruitful discussions. They are too numerous to be named here. We are also thankful for the support of Bahamian people and agencies, in particular the Gerace Research Center on San Salvador and the former Caribbean Marine Research Center on Lee Stocking Island. We thank the Editor Brian Jones and two anonymous reviewers who made constructive comments on an earlier version of this paper.

Appendix A. Type sections of the Whale Point Formation

1. Location and history

The WPF stratotype (N25°27′28.94″; W76°37′09.98″) is a low hill located at about 2 km SSE of Whale Point, North Eleuthera (Fig. A.1). The western flank of this mount has been carved during the construction of the NNW-trending dirt track leading to Whale Point resulting in a ca. 3.5 m-high, 200 m-long road cut. The hill top is covered by sand and bushy vegetation, but exposures can also be found on its eastern (ocean) side due to marine erosion. First described by Hearty and Kindler (1995a), this section has subsequently been reexamined by Kindler and Hearty (1997), Hearty (1998), Tormey (1999), Panuska et al. (2002), Brentini (2008), Nawratil de Bono (2008), and Kindler et al. (2010).

The WPF parastratotype (N25°25′56.90″; W76°35′51.63″) is a ca. 75 m-wide embayment on the ocean-facing shoreline of North Eleuthera, situated at about 800 m to the SE of the Glass Window Bridge (Fig. A.1). The appellation "Boiling Hole" is not reported on the official topographic chart of the area, but figured on numerous tourist maps when geological investigations began on Eleuthera in the late 1980's. This name is thus commonly used in the scientific literature (see references below), although the place is now called "Queen's Bath" on Google Map. Initially described by Hearty and Kindler (1993b), this exposure has been revisited by Hearty and Kindler (1995a), Kindler and Hearty (1995, 1997), Hearty (1998), Tormey (1999), Panuska et al. (2002), Kindler and Hine (2009), and Kindler et al. (2008, 2010).

2. Section description

Both sections expose four vertically stacked lithostratigraphic units (from bottom to top): the Owl's Hole (OHF), the Grotto Beach (GBF), the Whale Point, and the Rice Bay (RBF) formations (Table 1).

2.1. The Whale Point section

On the west side of the aforementioned hill, the GBF is exposed from road level (elevation +8 m) to a maximum height of about 1.2 m in the SE portion of the outcrop, but thins out towards the NW. It consists of fine-grained, well-sorted, whitish oolitic-peloidal grainstones showing high-angle cross beds with apparent dips towards both the NW and the SE and a few rhizoliths (Fig. A.2a). On the ocean side, the GBF overlies the OHF (Fig. A.2b). It is coarser grained, contains a high percentage of bioclasts, and exposes trough cross beds overlain by fenestrae-rich, lowangle cross strata with a seaward dip (Fig. A.2c). The upper boundary of the GBF corresponds to a corrugated surface (reliefs of up to 30 cm) overlain by a thin (<1 cm) micritic crust. Hearty (1998) retrieved an A/I ratio of 0.395 \pm 0.002 from the GBF at this location. The beds exposed on the road side can be interpreted as an eolianite based on the fine grain size, the good sorting, the occurrence of rhizoliths and of high-angle cross beds, whereas sedimentary structures on the ocean side characterize a shallowing-upward succession from subtidal to beach settings. Because the GBF is partly covered by the WPF at this location, it is not possible to figure out whether the beach on the ocean side and the eolianite on the road side are genetically related or if they represent distinct depositional events, possibly originating from different sources (i.e., lagoon versus open ocean; Kindler and Hine, 2009). The corrugated upper surface of the GBF has been identified as a "well-developed epikarst" (Panuska et al., 2002), and the overlying micritic crust corresponds to a pedogenic calcrete (Wright, 1994). The A/I ratio measured at this location is consistent with the MIS 5e age of the GBF.

The GBF is separated from the overlying WPF by a thin (10 to 40 cm) breccia layer sloping towards the NNW (Fig. A.2a), and comprising cmto dm-sized clasts, rhizoliths and Cerion snails in a light brown to pink (10YR 7/4) sandy matrix. The clasts locally show a fitted fabric, and consist of partly micritized oolitic-peloidal grainstone similar to the rocks forming the GBF below. In contrast, the matrix is made up of skeletal debris including fragments of red algae, mollusks and benthic foraminifers. Grains are generally coated by clay and micrite, occasionally linked by needle-fiber calcite cement, and locally aggregated as crumbs. Spherulites possibly produced by earth worms have also been observed in thin section. This breccia layer can be interpreted as a paleosol based on the occurrence of *Cerion* snails and rhizoliths, on the fitted fabric of clasts, and on the microfacies of the matrix. Nawratil de Bono (2008) classified this layer as a "calcareous paleosol" because the percentage of clay is very low. Its skeletal composition shows that the soil matrix is not derived from the underlying GBF, but from material accumulated during a younger depositional phase (i.e., in the latest MIS 5e or 5c; Nawratil de Bono, 2008; Brentini, 2008).

Due to the dip of the underlying paleosol, the thickness of the WPF varies between 3.5 m in the northern extremity of the exposure to 2 m in the south. The formation consists of a light-brown, friable bioclastic calcarenite with a grey alteration colour (refer to Section 4.4.3. for a detailed description of the microfacies). The lower portion of the unit shows high-angle cross-beds dipping towards the SE, whereas the

upper part is characterized by m-scale rhizocretions. Most samples collected from the upper part of this unit reveal needle-fiber calcite cements, root-hair sheaths and alveolar septal structures in thin section. The upper boundary of the WPF is a grooved surface with pits up to 60 cm deep capped by a thin micritic crust. Hearty (1998) retrieved an A/I ratio of 0.309 \pm 0.001 from the WPF at this locality. As previously discussed, the sedimentary structures and the diagenetic textures both lead to interpreting the WPF as an eolianite. The grooved surface is of karstic origin and the overlying micritic crust is pedogenic. The obtained A/I ratio is consistent with a MIS 5a age (Hearty and Kaufman, 2000, 2009).

The WPF is overlain by a thin (5 to 60 cm) breccia layer comprising cm- to dm-sized skeletal clasts and rhizocretions in a reddish matrix consisting of clay and coarse bioclastic sands. This layer, interpreted as a paleosol formed at the expense of the WPF (Nawratil de Bono, 2008), is locally covered by subrecent bioclastic sand (RBF). A detailed log of the WPF stratotype is published in Hearty (1998) and Nawratil de Bono (2008).

2.2. The Boiling Hole Section

The most detailed descriptions of the Boiling Hole section can be found in Kindler and Hearty (1995), Hearty (1998), Tormey (1999), Kindler and Hine (2009) and Kindler et al. (2008, 2010). The complexity of the exposure, its size (Fig. A.3a) and the numerous possibilities of logging sites explain the minor discrepancies that may be found between these descriptions. The main points to remember are the following: (1) the GBF occurs in a large interdune swale between two karstified, paleosol-capped eolianites correlated with the OHF (Fig. A.3a); (2) of variable thickness, the GBF consists of oolitic-peloidal grainstones including a small, but remarkable proportion of radial ooids, and comprises two shallowing-upward depositional sequences from subtidal

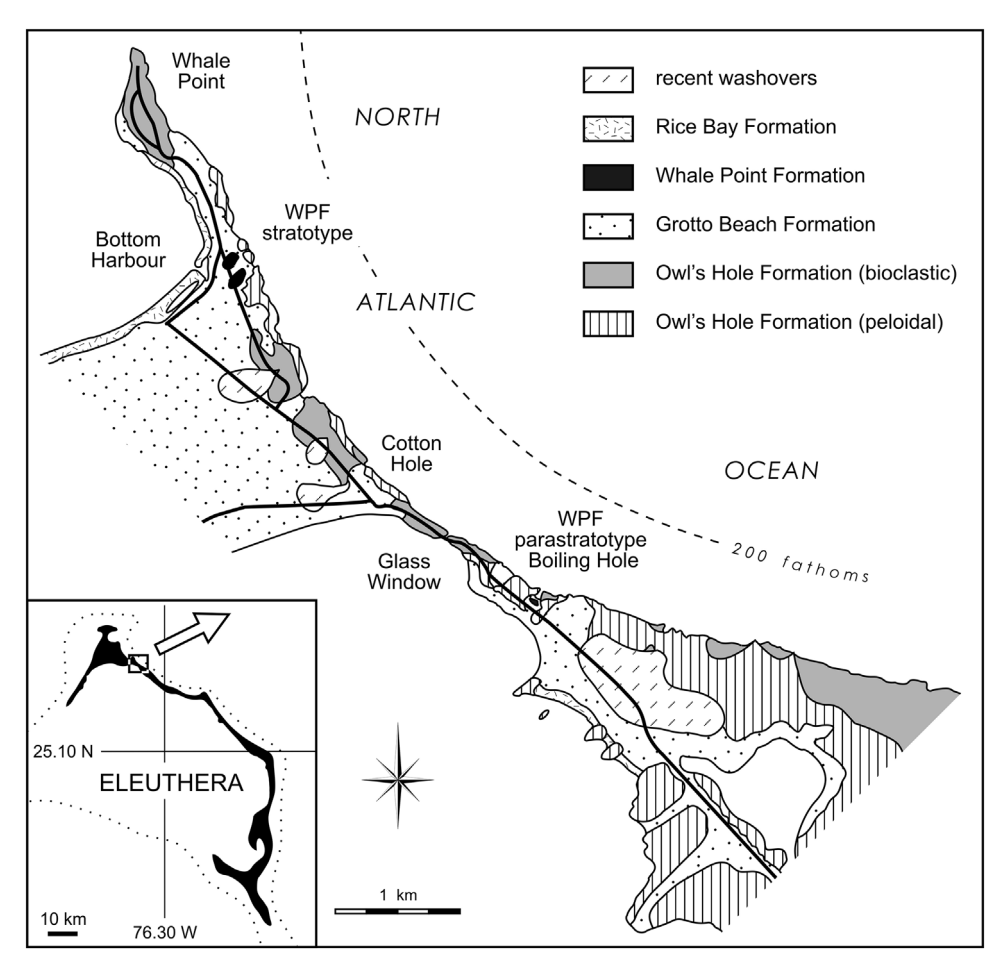


Fig. A.1. Geological map of the Glass Window area (North Eleuthera) showing the location of the type sections of the WPF (modified from Kindler and Hearty, 1997).



Fig. A.2. A. Whale Point section (western side of the hill, along the dirt road). The WPF and GBF eolianites are vertically stacked and separated by a ca. 30 cm-thick carbonate paleosol. Note large-scale foresets with an apparent dip towards the SSE in the GBF. Person on the left side of the group is 1.60 m tall. B. Whale Point section (eastern side, along the ocean) showing the vertical stacking of the OHF, GBF and WPF. White square corresponds to panel c. Person on the left is 1.85 m tall. C. Similar view as panel a. Red arrow points to the paleosol separating the WPF from the GBF. The latter formation is represented by low-angle, seaward dipping strata (i.e., beach beds). Coarse conglomerate in the foreground is recent storm rubble. Person for scale is 1.75 m tall.

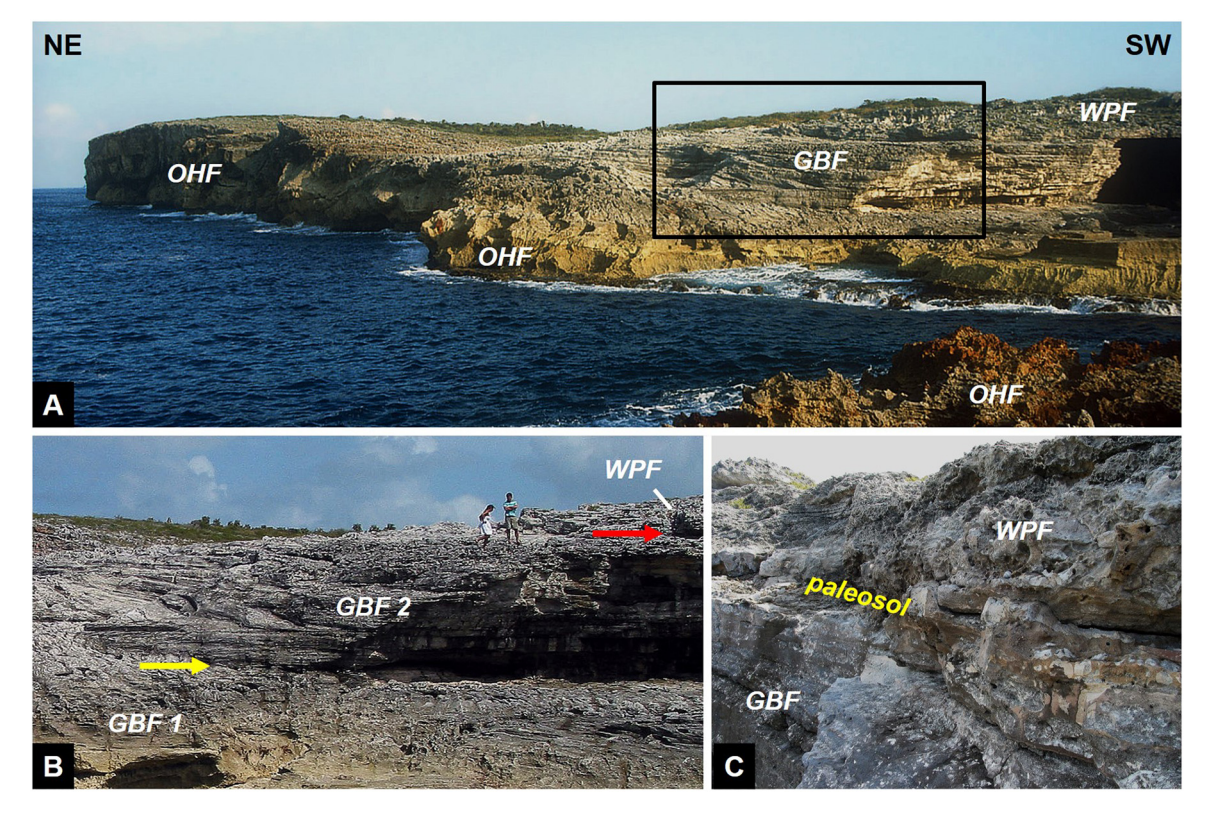


Fig. A.3. A. Southeastern end of the Boiling Hole cove exposing the vertical stacking of the OHF (Middle Pleistocene), the GBF (MIS 5e) and the WPF (MIS 5a). Black rectangle shows the position of panel b. Background cliff height is 20 m; (modified from Kindler and Hearty, 1995). B. Close-up view showing the two depositional sequences of the GBF (boundary designated by the yellow arrow) overlain by the WPF. Red arrow points to the GBF/WPF boundary. Standing person is 1.80 m tall. C. Detail of the GBF/WPF boundary in the upper part of the Boiling Hole exposure. The intervening, breccia-rich paleosol is 30 cm thick.

P. Kindler and P.J. Hearty Sedimentary Geology 432 (2022) 106107

to eolian separated by an erosional surface (Fig. A.3b); (3) these sediments were transported from the bank interior, and are now exposed on the ocean side due to coastal retreat; (4) the GBF yielded an A/I ratio of 0.407 \pm 0.003 which is consistent with a MIS 5e age (Hearty, 1998); (5) the upper surface of this formation is of karstic origin, and is capped by a cm-thick pedogenic calcrete locally overlain by a breccia-rich paleosol (Fig. A.3c); (6) the WPF overlies both the GBF and the OHF (Fig. A.3a); (7) it forms up to 3 m-high bioclastic eolianites bearing abundant rhizoliths, and it is capped by a pedogenic calcrete; (8) the WPF gave an A/I ratio of 0.302 \pm 0.003 which agrees with a MIS 5a age (Hearty, 1998); (9) the calcrete-capped WPF is overlain by subrecent skeletal sand in the landward part of the exposure.

References

- Alonso-Zarza, A.M., Genise, J.F., Cabrera, M.C., Mangas, J., Martin-Pérez, A., Valdeolmillos, A., Dorado-Valiño, M., 2008. Megarhizoliths in Pleistocene eolian deposits from Gran Canaria (Spain): Ichnological and palaeoenvironmental significance. Paleogeography, Paleoclimatology, Paleoecology 265, 39–51.
- Austermann, J., Mitrovica, J.X., Huybers, P., Rovere, A., 2017. Detection of a dynamic topography signal in last interglacial sea-level records. Science Advances 3. https://doi.org/10.1126/sciadv.1700457.
- Bahamas Government, 1969. Topographic Map, Eleuthera, Sheet 3, Scale 1:25,000.
- Bathurst, R.G.C., 1975. Carbonate Sediments and their Diagenesis. Developments in Sedimentology 12. Elsevier, Amsterdam, NL (658 pp.).
- Beck, H.E., Zimmermann, N.E., McVicar, T.R., Vergopolan, N., Berg, A., Wood, E.F., 2018. Present and future Köppen-Geiger climate classification maps at 1-km resolution. Nature Scientific Data 5, 180214. https://doi.org/10.1038/sdata.2018.214.
- Beier, J.A., 1987. Petrographic and geochemical analysis of caliche profiles in a Bahamian Pleistocene dune. Sedimentology 34, 991–998.
- Berger, A.L., 1978. Long-term variations of caloric insolation resulting from the Earth's orbital elements. Quaternary Research 9, 139–167.
- Bergman, K.L., Westphal, H., Janson, X., Poiriez, A., Eberli, G.P., 2010. Controlling parameters on facies geometries of the Bahamas, an isolated carbonate platform environment. In: Westphal, H., Riegl, B., Eberli, G.P. (Eds.), Carbonate Depositional Systems: Assessing Dimensions and Controlling Parameters. The Bahamas, Belize and the Persian/Arabian Gulf. Springer Verlag, Berlin, pp. 5–80.
- Boardman, M.R., Neumann, A.C., Rasmussen, K.A., 1989. Holocene Sea Level in the Bahamas. In: Mylroie, J.E. (Ed.), Proceedings of the Fourth Symposium on the Geology of the Bahamas. 17–22 June, 1988. Bahamian Field Station, San Salvador, pp. 45–52.
- Bowen, D.Q., 1988. Quaternary Geology. A stratigraphic framework for multidisciplinary work. Pergamon Press, Oxford, England (237 pp.).
- Brentini, M., 2008. Pétrographie sédimentaire et géochimie isotopique de paléosols et d'éolianites d'Eleuthera (Bahamas) d'âge Pléistocène supérieur à Holocène. Implication sur la paléo-circulation atmosphérique. (M.Sc. Thesis)University of Geneva, Geneva, Switzerland (115 pp.) (in French with English abstract).
- Bretz, J.H., 1960. Bermuda: a partially drowned, late mature, Pleistocene karst. Geological Society of America Bulletin 71, 1729–1754.
- Brown, T.W., 1984. Formation and development of caliche profile in eolian deposits: San Salvador, The Bahamas. In: Teeter, J.W. (Ed.), Proceedings of the Second Symposium on the Geology of the Bahamas. 16-20 June 1984. Bahamian Field Station, San Salvador, Bahamas, pp. 245–264.
- Carew, J.L., Mylroie, J.E., 1985. The Pleistocene and Holocene stratigraphy of San Salvador Island, Bahamas, with reference to marine and terrestrial lithofacies at French Bay. In: Curran, H.A. (Ed.), Pleistocene and Holocene Carbonate Environments on San Salvador Island, Bahamas Guidebook for Geological Society of America, Orlando Annual Meeting Field Trip. CCFL Bahamian Field Station, Ft. Lauderdale, FL, pp. 11–61.
- Carew, J.L., Mylroie, J.E., 1994. Discussion of: Hearty, P.J. and Kindler, P., 1993. New perspectives on Bahamian Geology: San Salvador, Bahamas. Journal of Coastal Research, 9, 577-594. Journal of Coastal Research 10, 1087–1094.
- Carew, J.L., Mylroie, J.E., 1995a. A stratigraphic and depositional model for the Bahama Islands. In: Curran, H.A., White, B. (Eds.), Terrestrial and Shallow Marine Geology of the Bahamas and Bermuda. Geological Society of America Special Paper300, pp. 5–31 (Boulder, CO, USA).
- Carew, J.L., Mylroie, J.E., 1995b. Rejoinder to: Hearty, P.J. and Kindler, P., 1994. Reply-Straw Men, Glass Houses, Apples and Oranges: a response to Carew and Mylroie's comment on Hearty and Kindler (1993). Journal of Coastal Research, 10, 1095– 1105. Journal of Coastal Research 11, 256–260.
- Carew, J.L., Mylroie, J.E., 1997. Geology of the Bahamas. In: Vacher, H.L., Quinn, T.M. (Eds.), Geology and Hydrogeology of Carbonate Islands. Developments in Sedimentology54. Elsevier, Amsterdam, NL, pp. 91–139.
- Carew, J.L., Mylroie, J.E., 2001. Quaternary carbonate eolianites of the Bahamas: Useful analogs for the interpretation of ancient rocks? In: Abegg, F.E., Loope, D.B., Harris, P.M. (Eds.), Modern and Ancient Carbonate Eolianites: Sedimentology, Sequence Stratigraphy, and Diagenesis. SEPM Special Publication71, pp. 33–45 (Tulsa, OK)
- Chen, J.H., Curran, H.A., White, B., Wasserburg, G.J., 1991. Precise chronology of the last interglacial period; ²³⁴U-²³⁰Th data from fossil coral reefs in the Bahamas. Geological Society of America Bulletin 103, 82–97.
- Coyne, M.K., Jones, B., Ford, D., 2007. Highstands during Marine Isotope Stage 5: evidence from the Ironshore Formation of Grand Cayman, British West Indies. Quaternary Science Reviews 26, 536–559.

Creveling, J.R., Mitrovica, J.X., Clark, P.U., Waelbroeck, C., Pico, T., 2017. Predicted bounds on peak global mean sea level during marine isotope stages 5a and 5c. Quaternary Science Reviews 163, 193–208.

- Dansgaard, W., Johnsen, S.J., Clausen, H.B., Dahl-Jensen, D., Gundestrup, N.S., Hammer, C.U., Hvidberg, C.S., Steffensen, J.P., Sveinbjörnsdottir, A.E., Jouzel, J., Bond, G., 1993. Evidence for general instability of past climate from a 250-kyr ice-core record. Nature 364, 218–220.
- Davaud, E., Strasser, A., 1984. Progradation, cimentation, érosion: évolution sédimentaire et diagénétique récente d'un littoral carbonaté (Bimini, Bahamas). Eclogae Geologicae Helvetiae 77, 449–468 (in French with English abstract).
- Dorale, J.A., Onac, B.P., Fornos, J.J., Ginés, J., Ginés, A., Tuccimei, P., Peate, D.W., 2010. Sealevel highstand 81,000 years ago in Mallorca. Science 327, 860–863.
- Dravis, J.J., 1996. Rapidity of freshwater calcite cementation implications for carbonate diagenesis and sequence stratigraphy. Sedimentary Geology 107, 1–10.
- Dravis, J.J., Wanless, H.R., 2017. Impact of strong easterly trade winds on carbonate petroleum exploration - relationships developed from Caicos Platform, southeastern Bahamas. Marine and Petroleum Geology 85, 272–300.
- Dutton, A., Lambeck, K., 2012. Ice volume and sea level during the last interglacial. Science 337, 216–219.
- Dutton, A., Carlson, A.E., Long, A.J., Milne, G.A., Clark, P.U., DeConto, R., Horton, B.P., Rahmstorf, S., Raymo, M.E., 2015. Sea-level rise due to polar ice-sheet mass loss during past warm periods. Science 349 (6244), aaa4019. https://doi.org/10.1126/science. aaa4019.
- Friedman, G.M., 1998. Rapidity of marine carbonate cementation implications for carbonate diagenesis and sequence stratigraphy: perspective. Sedimentary Geology 119, 1–4.
- Garrett, P., Gould, S.J., 1984. Geology of New Providence Island, Bahamas. Geological Society of America Bulletin 95, 209–220.
- Gerhardt, G., 1983. The Anatomy and History of a Pleistocene Strand Plain Deposit. Grand Bahama Island; Bahamas (M.Sc. Thesis). University of Miami, Miami, FL, USA (131 pp.).
- Gibson, K.A., Peterson, L.C., 2014. A 0.6 million year record of millenial-scale climate variability in the tropics. Geophysical Research Letters 41, 969–975.
- Gischler, E., Möder, A., 2009. Modern benthic foraminifera on Banco Chinchorro, Quintana Roo, Mexico. Facies 55, 27–35.
- Godefroid, F., 2012. Géologie de Mayaguana, SE de l'archipel des Bahamas. Terre & Environnement108 pp. 1–230 (in French with English abstract).
- Godefroid, F., Kindler, P., 2016. Prominent geological features of Crooked Island, SE Bahamas. In: Glumac, B., Savarese, M. (Eds.), Proceedings of the 16th Symposium on the Geology of the Bahamas and Other Carbonate Regions. 14-18 June 2012. Gerace Research Center, San Salvador, Bahamas, pp. 26–38.
- Godefroid, F., Kindler, P., Chiaradia, M., Fischer, G., 2019. The misery Point cliff, Mayaguana Island, SE Bahamas: a unique record of sea-level highstands since the early Pleistocene. Swiss Journal of Geosciences 112, 287–305.
- Gould, S.J., 1997. The taxonomy and geographic variation of Cerion on San Salvador (Bahama Islands). In: Carew, J.L. (Ed.), Proceedings of the Eighth Symposium on the Geology of the Bahamas and Other Carbonate Regions. 30 May 3 June 1996. Bahamian Field Station, San Salvador, Bahamas, pp. 73–91.
- Grammer, G.M., Ginsburg, R.N., McNeill, D.F., 1991. Morphology and development of modern carbonate foreslopes, Tongue of the Ocean, Bahamas. In: Larue, D.K., Draper, G. (Eds.), Transactions of the 12th Caribbean Geological Conference, 7–11 August 1989, St. Croix, U.S. Virgin Islands. Miami Geological Society, pp. 27–32.
- Hallock, P., Glenn, E.C., 1986. Larger foraminifera: a tool for paleoenvironmental analysis of Cenozoic carbonate depositional facies. Palaios 1, 55–64.
- Harmon, R.S., Mitterer, R.M., Kriausakul, N., Land, L.S., Schwarcz, H.P., Garrett, P., Larson, G.J., Vacher, H.L., Rowe, M., 1983. U-series and amino-acid racemization geochronology of Bermuda: implications for eustatic sea-level fluctuation over the past 250,000 years. Paleogeography, Paleoclimatology, Paleoecology 44, 41–70.
- Harris, P.M., Purkis, S.J., Ellis, J., Swart, P.K., Reijmer, J.J.G., 2015. Mapping bathymetry and depositional facies on Great Bahama Bank. Sedimentology 62, 566–589.
- Harris, P.M., Diaz, M.R., Eberli, G.P., 2019. The formation and distribution of modern ooids on Great Bahama Bank. Annual Review of Marine Science 11, 491–516.
- Hearty, P.J., 1998. The geology of Eleuthera Island, Bahamas: a rosetta stone of Quaternary Stratigraphy and sea-level history. Quaternary Science Reviews 17, 333–355.
- Hearty, P.J., 2002. Revision of the late Pleistocene stratigraphy of Bermuda. Sedimentary Geology 153, 1–21.
- Hearty, P.J., 2010. Chronostratigraphy and morphological changes in *Cerion* land snail shells over the past 130 ka on Long Island, Bahamas. Quaternary Geochronology 5, 50–64.
- Hearty, P.J., Kaufman, D.S., 2000. Whole-rock aminostratigraphy and Quaternary Sea-level history of the Bahamas. Quaternary Research 54, 163–173.
- Hearty, P.J., Kaufman, D.S., 2009. A *Cerion*-based chronostratigraphy and age model from the central Bahama Islands: amino acid racemization and ¹⁴C in land snails and sediments. Quaternary Geochronology 4, 148–159.
- Hearty, P.J., Kindler, P., 1993a. New perspectives on Bahamian geology: San Salvador Island, Bahamas. Journal of Coastal Research 9, 577–594.
- Hearty, P.J., Kindler, P., 1993b. An illustrated stratigraphy of the Bahamas: in search of a common origin. Bahamas Journal of Science 1, 28–45.
- Hearty, P.J., Kindler, P., 1994. Straw Men, Glass Houses, Apples and Oranges: a response to Carew and Mylroie's comment on Hearty and Kindler (1993). Journal of Coastal Research 10, 1095–1104.
- Hearty, P.J., Kindler, P., 1995a. The geology of North Eleuthera, Bahamas: a "rosetta stone" of Quaternary stratigraphy and sea levels. Field Trip #3 Guidebook, First SEPM Congress on Sedimentary Geology. 13–16 August 1995, St. Pete Beach, FL, USA (23 pp.).
- Hearty, P.J., Kindler, P., 1995b. Sea-level highstand chronology from stable carbonate platforms (Bermuda and the Bahamas). Journal of Coastal Research 11, 675–689.

P. Kindler and P.J. Hearty Sedimentary Geology 432 (2022) 106107

Hearty, P.J., Kindler, P., 1997. The stratigraphy and surficial geology of New Providence and surrounding islands, Bahamas, Journal of Coastal Research 13, 798–812.

- Hearty, P.J., Schellenberg, S.A., 2008. Integrated Late Quaternary chronostratigraphy for San Salvador Island, Bahamas: patterns and trends of morphological change in the land snail *Cerion*. Paleogeography, Paleoclimatology, Paleoecology 267, 41–58.
- Hearty, P.J., Vacher, H.L., Mitterer, R.M., 1992. Aminostratigraphy and ages of Pleistocene limestones of Bermuda. Geological Society of America Bulletin 104, 471–480.
- Hearty, P.J., Kindler, P., Schellenberg, S.A., 1993. The late Quaternary evolution of surface rocks on San Salvador Island, Bahamas. In: White, B. (Ed.), Proceedings of the Sixth Symposium on the Geology of the Bahamas. 11-15 June 1992. Bahamian Field Station, San Salvador, Bahamas, pp. 205–222.
- Hesp, P.A., Dillenburg, S.R., Barboza, E.G., Tomazelli, L.J., Ayup-Zouain, R.N., Esteves, L.S., Gruber, N.L.S., Toldo-Jr, E.E., De A. Tabajara, L.L.C., Clerot, L.C.P., 2005. Beach ridges, foredunes or transgressive dunefields? Definitions and an examination of the Torres to Tramandai barrier system, Southern Brazil. Annals of the Brazilian Academy of Sciences 77, 493–508.
- Hine, A.C., 1977. Lily Bank, Bahamas: history of an active oolite sand shoal. Journal of Sedimentary Petrology 47, 1554–1581.
- Hine, A.C., Steinmetz, J.C., 1984. Cay Sal Bank, Bahamas a partially drowned carbonate platform. Marine Geology 59, 135–164.
- Hunter, R.E., 1977. Basic types of stratification in small eolian dunes. Sedimentology 24, 361–387.
- Itzhaki, Y., 1961. Pleistocene shorelines in the coastal plains of Israel. Geological Survey of Israel Bulletin 32, 1–9.
- Jackson, K.L., 2017. Sedimentary Record of Holocene and Pleistocene Sea-Level Oscillations in the Exuma Cays and New Providence, Bahamas. (Ph.D. thesis)University of Miami, Miami, FL, USA (506 pp.).
- James, N.P., Jones, B., 2015. Origin of Carbonate Sedimentary Rocks. John Wiley & Sons, Chichester, UK (464 pp.).
- Kelley, K.N., Mylroie, J.E., Mylroie, J.R., Moore, C.M., Collins, L.R., Ersek, L., Lascu, I., Roth, M.J., Moore, P.J., Passion, R., Shaw, C., 2011. Eolianites and Karst Development in the Mayan Riviera, Mexico. Speleogenesis & Evolution of Karst Aquifers11 pp. 32–39.
- Kerans, C., Zahm, C., Bachtel, S.L., Hearty, P.J., Cheng, H., 2019. Anatomy of a late Quaternary carbonate island: Constraints on timing and magnitude of sea-level fluctuations, West Caicos, Turks and Caicos Islands, BWI. Quaternary Science Reviews 205, 193–223
- Kindler, P., 1995. New data on the Holocene stratigraphy of Lee Stocking Island (Bahamas) and its relation to sea-level history. In: Curran, H.A., White, B. (Eds.), Terrestrial and Shallow Marine Geology of the Bahamas and Bermuda. Geological Society of America Special Paper 300, Boulder, CO, USA, pp. 105–116.
- Kindler, P., Hearty, P.J., 1995. Pre-Sangamonian eolianites in the Bahamas? New evidence from Eleuthera Island. Marine Geology 127, 73–86.
- Kindler, P., Hearty, P.J., 1996. Carbonate petrography as an indicator of climate and sealevel changes: new data from Bahamian Quaternary units. Sedimentology 43, 281, 200
- Kindler, P., Hearty, P.J., 1997. Geology of the Bahamas: Architecture of Bahamian Islands. In: Vacher, H.L., Quinn, T.M. (Eds.), Geology and Hydrogeology of Carbonate Islands. Developments in Sedimentology 54. Elsevier, Amsterdam, NL, pp. 141–160.
- Kindler, P., Hine, A.C., 2009. The paradoxical occurrence of oolitic limestone on the eastern islands of Great Bahama Bank: Where do the ooids come from? In: Swart, P.K., Eberli, G.P., McKenzie, J.A. (Eds.), Perspectives in Carbonate Geology. A Tribute to the Career of Robert Nathan Ginsburg. IAS Special Publication41. John Wiley & Sons, Chichester, UK, pp. 113–122
- Kindler, P., Mazzolini, D., 2001. Sedimentology and petrography of dredged carbonate sands from Stocking Island (Bahamas). Implications for meteoric diagenesis and eolianite formation. Paleogeography, Paleoclimatology, Paleoecology 175, 369–379.
- Kindler, P., Curran, H.A., Marty, D., Samankassou, E., 2008. Multiple sedimentary sequences, bird tracks and lagoon beaches in last interglacial oolites, Boiling Hole, North Eleuthera, Bahamas. In: Park, L., Freile, B. (Eds.), Proceedings of the 13th Symposium on the Geology of the Bahamas and Other Carbonate Regions. 8-12 June 2006. Gerace Research Center, San Salvador, Bahamas, pp. 169–181.
- Kindler, P., Mylroie, J.E., Curran, H.A., Carew, J.L., Gamble, D.W., Rothfus, T.A., Savarese, M., Sealey, N.E., 2010. Geology of Central Eleuthera, Bahamas: A Field Trip Guide. 15th Symposium on the Geology of the Bahamas and Other Carbonate Regions. Gerace Research Centrer, San Salvador, Bahamas (75 pp.).
- Kindler, P., Godefroid, F., Chiaradia, M., Ehlert, C., Eisenhauer, A., Frank, M., Hasler, C.-A., Samankassou, E., 2011. Discovery of Miocene to early Pleistocene deposits on Mayaguana, Bahamas: evidence for recent active tectonism on the north American margin. Geology 39, 523–526.
- Klappa, C.F., 1980. Rhizoliths in terrestrial carbonates: classification, recognition, genesis and significance. Sedimentology 27, 613–629.
- Land, L.S., MacKenzie, F.T., Gould, S.J., 1967. Pleistocene history of Bermuda. Geological Society of America Bulletin 78, 993–1006.
- Lees, A., Buller, A.T., 1972. Modern temperate-water and warm-water shelf carbonate sediments contrasted. Marine Geology 13, 67–73.
- Li, C., Jones, B., 1997. Comparison of foraminiferal assemblages in sediments on the windward and leeward shelves of Grand Cayman, British West Indies. Palaios 12, 12–26.
- Li, W.-X., Lundberg, J., Dickin, A.P., Ford, D.C., Schwarcz, H.P., McNutt, R., Williams, D., 1989. High-precision mass-spectrometric uranium-series dating of cave deposits and implications for palaeoclimate studies. Nature 339, 534–536.
- Loucks, R.G., Ward, W.C., 2001. Eolian stratification and beach-to-dune transition in a Holocene carbonate eolianite complex, Isla Cancun, Quintana Roo, Mexico. In: Abegg, F.E., Loope, D.B., Harris, P.M. (Eds.), Modern and Ancient Carbonate Eolianites: Sedimentology, Sequence Stratigraphy, and Diagenesis. SEPM Special Publication71, pp. 57–76 (Tulsa, OK).

- Ludwig, K.R., Muhs, D.R., Simmons, K.R., Halley, R.B., Shinn, E.A., 1996. Sea-level records at ~80 ka from tectonically stable platforms: Florida and Bermuda. Geology 24, 211–214.
- Lundberg, J., Ford, D.C., 1994. Late Pleistocene Sea level change in the Bahamas from mass spectrometric U-series dating of submerged speleothem. Quaternary Science Reviews 13. 1–14.
- Lynts, G.W., 1970. Conceptual model of the Bahamian platform for the last 135 million years. Nature 225, 1226–1228.
- Martin, A.J., Stearns, D., Whitten, M.J., Hage, M.M., Page, M., Basu, A., 2020. First known trace fossil of a nesting iguana (Pleistocene), The Bahamas. PLoS ONE 15, e0242935. https://doi.org/10.1371/journal.pone.0242935.
- Masaferro, J.L., Eberli, G.P., 1999. Jurassic-Cenozoic structural evolution of the southern Great Bahama Bank. In: Mann, P. (Ed.), Caribbean Basins (Sedimentary Basins of the World). Elsevier, Amsterdam, NI, pp. 167–193.
- Mauz, B., Hijma, M.P., Amorosi, A., Porat, N., Galili, E., Bloemendal, J., 2013. Eolian beach ridges and their significance for climate and sea level: concept and insight from the Levant coast (East Mediterranean). Earth Science Reviews 121, 31–54.
- Mazzolini, D., 2000. Cartographie géologique et stratigraphie physique de Stocking Island, Bahamas. (M.Sc. thesis)University of Geneva, Geneva, Switzerland (70 pp.) (in French with English abstract).
- Miller, J., 1988. Microscopical techniques: I. Slices, slides, stains and peels. In: Tucker, M. (Ed.), Techniques in Sedimentology. Blackwell Scientific Publications, Oxford, UK, pp. 86–107.
- Muhs, D.R., Bush, C.A., Stewart, K.C., Rowland, T.R., Crittenden, R.C., 1990. Geochemical evidence of Saharan dust parent material for soils developed on Quaternary limestones of Caribbean and Western Atlantic islands. Quaternary Research 33, 157–177.
- Muhs, D.R., Simmons, K.R., Steinke, B., 2002. Timing and warmth of the last Interglacial period: new U-series evidence from Hawaii and Bermuda and a new fossil compilation for North America. Quaternary Science Reviews 21, 1355–1383.
- Muhs, D.R., Simmons, K.R., Schumann, R.R., Schweig, E.S., Rowe, M.P., 2020. Testing glacial isostatic adjustment models of last-interglacial sea level history in the Bahamas and Bermuda. Ouaternary Science Reviews 233. 106212.
- Mulder, T., Ducassou, E., Gillet, H., Hanquiez, V., Tournadour, E., Combes, J., Eberli, G.P., Kindler, P., Gonthier, E., Conesa, G., Robin, C., Sianipar, R., Reijmer, J.J.G., François, A., 2012. Canyon morphology on a modern carbonate slope of the Bahamas: evidence of regional tectonic tilting. Geology 40, 771–774.
- Mullins, H.T., Van Buren, H.M., 1981. Walkers Cay Fault, Bahamas: evidence for Cenozoic faulting. Geo-Marine Letters 1, 225–231.
- Mullins, H.T., Dolan, J., Breen, N., Andersen, B., Gaylord, M., Petruccione, J.L., Wellner, R.W., Melillo, A.J., Jurgens, A.D., 1991. Retreat of carbonate platforms: response to tectonic processes. Geology 19, 1089–1092.
- Mullins, H.T., Breen, N., Dolan, J., Wellner, R.W., Petruccione, J.L., Gaylord, M., Andersen, B., Melillo, A.J., Jurgens, A.D., Orange, D., 1992. Carbonate platforms along the southeast Bahamas-Hispaniola collision zone. Marine Geology 105, 169–209.
- Murray-Wallace, C.V., Belperio, A.P., Dosseto, A., Nicholas, W.A., Mitchell, C., Bourman, R.P., Eggins, S.M., Grün, R., 2016. Last interglacial (MIS 5e) sea-level determined from a tectonically stable, far-field location, Eyre Peninsula, southern Australia. Australian Journal of Earth Sciences 63, 611–630.
- Mutti, M., Hallock, P., 2003. Carbonate systems along nutrient and temperature gradients: some sedimentological and geochemical constraints. International Journal of Earth Sciences 92, 465–475.
- Mylroie, J.E., 2008. Late Quaternary Sea-level position: evidence from Bahamian carbonate deposition and dissolution cycles. Quaternary International 183, 61–75.
- Mylroie, J.E., Lace, M.J., Albury, N.A., Mylroie, J.R., 2020. Flank margin caves and the position of Mid- to Late Pleistocene Sea level in the Bahamas. Journal of Coastal Research 36, 249–260.
- Nawratil de Bono, C.F., 2008. Pétrographie, micromorphologie et minéralogie des paleosols pléistocènes d'Eleuthera, Bahamas : enseignements paléoclimatiques, stratigraphiques et sédimentologiques. Terre & Environnement75 pp. 1–226 (in French with English abstract).
- North Greenland Ice Core Project, 2004. High-resolution record of Northern Hemisphere climate extending into the last interglacial period. Nature 431, 147–151.
- Opdyke, N.D., Spangler, D.P., Smith, D.L., Jones, D.S., Linquist, R.C., 1984. Origin of the epeirogenic uplift of Pliocene-Pleistocene beach ridges in Florida and development of the Florida karst. Geology 12, 226–228.
- Panuska, B.C., Boardman, M.R., Carew, J.L., Mylroie, J.E., Sealey, N.E., Voegeli, V., 2002. Eleuthera Island Field Trip Guide. 11th Symposium on the Geology of the Bahamas and Other Carbonate Region. Gerace Research Centrer, San Salvador, Bahamas (20 pp.).
- Peterson, L.C., Haug, G.H., Hughen, K.A., Röhl, U., 2000. Rapid changes in the hydrologic cycle of the tropical Atlantic during the last glacial. Science 290, 1947–1951.
- Playton, T.E., Janson, X., Kerans, C., 2010. Carbonate slopes. In: James, N.P., Dalrymple, R.W. (Eds.), Facies Models 4. GEOtext 6. Geological Association of Canada, pp. 449–476.
- Potter, E.-K., Lambeck, K., 2003. Reconciliation of sea-level observations in the Western North Atlantic during the last glacial cycle. Earth and Planetary Science Letters 217, 171–181.
- Potter, E.-K., Esat, T.M., Schellmann, G., Radtke, U., Lambeck, K., McCulloch, M.T., 2004. Suborbital-period Sea-level oscillations during marine isotope substages 5a and 5c. Earth and Planetary Science Letters 225, 191–204.
- Railsback, L.B., Gibbard, P.L., Head, M.J., Voarintsoa, N.R.G., Toucanne, S., 2015. An optimized scheme of lettered marine isotope substages for the last 1.0 million years, and the climatostratigraphic nature of isotope stages and substages. Quaternary Science Reviews 111, 94–106.
- Rankey, E.C., Doolittle, D.F., 2012. Geomorphology of carbonate platform-marginal uppermost slopes: Insights from a Holocene analogue, Little Bahama Bank, Bahamas. Sedimentology 59, 2146–2171.

- Rankey, E.C., Reeder, S.L., 2011. Holocene oolitic marine sand complexes of the Bahamas. Journal of Sedimentary Research 81, 97–117.
- Rasmussen, S.O., Bigler, M., Blockley, S.P., Blunier, T., Buchardt, S.L., Clausen, H.B., Cvijanovic, I., Dahl-Jensen, D., Johnsen, S.J., Fischer, H., Gkinis, V., Guillevic, M., Hoek, W.Z., Lowe, J., Pedro, J.B., Popp, T., Seierstad, I.K., Steffensen, J.P., Svensson, A.M., Vallelonga, P., Vinther, B.M., Walker, M.J.C., Wheatley, J.J., Winstrup, M., 2014. A stratigraphic framework for abrupt climatic changes during the Last Glacial period based on three synchronized Greenland ice-core records: refining and extending the INTIMATE event stratigraphy. Quaternary Science Reviews 106, 14–28.
- Richards, D.A., Smart, P.L., Edwards, R.L., 1994. Maximum Sea levels for the last glacial period from U-series ages of submerged speleothems. Nature 367, 357–360.
- Rose, J., 1983. Variation of Cerion populations on San Salvador. In: Gerace, D.T. (Ed.), Proceedings of the First Symposium on the Geology of the Bahamas. 23-25 March 1982. CCFL Bahamas Field Station, San Salvador, Bahamas, pp. 42-44.
- Rose, P.R., Lidz, B., 1977. Diagnostic Foraminiferal Assemblages of Shallow-Water Modern Environments: South Florida and the Bahamas. Sedimenta VI. University of Miami, Miami, FL (55 pp.).
- Rowe, M.P., Bristow, C.S., 2015a. Landward-advancing Quaternary eolianites of Bermuda. Aeolian Research 19. 235–249.
- Rowe, M.P., Bristow, C.S., 2015b. Sea-level controls on carbonate beaches and coastal dunes (eolianite): Lessons from Pleistocene Bermuda. Geological Society of America Bulletin 127, 1645–1665.
- Sealey, N.E., 2006. Bahamian Landscapes. An Introduction to the Geology and Physical Geography of the Bahamas. Macmillan Publishers, Oxford, UK (174 pp.).
- Siddall, M., Rohling, E.J., Almogi-Labin, A., Hemleben, C., Meischner, D., Schmelzer, I., Smeed, D.A., 2003. Sea-level fluctuations during the last glacial cycle. Nature 423, 853–858.
- Spratt, R.M., Lisiecki, L.E., 2016. A late Pleistocene sea level stack. Climate of the Past 12, 1079–1092.
- Thompson, W.G., Curran, H.A., Wilson, M.A., White, B., 2011. Sea-level oscillations during the last interglacial highstand recorded by Bahamas corals. Nature Geoscience 4, 684–687.
- Tormey, B.R., 1999. Evidence of Rapid Climate Change during the Last Interglacial in Calcarenites of Eleuthera, Bahamas. (M.Sc. thesis)University of North Carolina (Chapel Hill), NC, USA (135 pp.).
- Toscano, M.A., Lundberg, J., 1999. Submerged late Pleistocene reefs on the tectonicallystable S.E. Florida margin: high-precision geochronology, stratigraphy, resolution of Substage 5a sea-level elevation, and orbital forcing. Quaternary Science Reviews 18, 753–767.
- Vacher, L., 1973. Coastal dunes of Younger Bermuda. In: Coates, D.R. (Ed.), Coastal Geomorphology. Publications in Geomorphology. State University of New York, NY, USA, pp. 355–391.
- Vacher, H.L., Hearty, P.J., 1989. History of stage 5 sea level in Bermuda: review with new evidence of a rise to present sea level during substage 5a. Quaternary Science Reviews 8, 159–168.

- Vacher, H.L., Rowe, M.P., 1997. Geology and hydrogeology of Bermuda. In: Vacher, H.L., Quinn, T.M. (Eds.), Geology and Hydrogeology of Carbonate Islands. Developments in Sedimentology54. Elservier, Amsterdam, NL, pp. 35–90.
- Vacher, H.L., Hearty, P.J., Rowe, M.P., 1995. Stratigraphy of Bermuda: Nomenclature, concepts and status of multiple systems of classification. In: Curran, H.A., White, B. (Eds.), Terrestrial and Shallow Marine Geology of the Bahamas and Bermuda. Geological Society of America Special Paper300, pp. 271–294 (Boulder, CO, USA).
- Vimpere, L., 2017. Stratigraphy and Sedimentology of Quaternary Carbonate Units around and within Dean's Blue Hole, Long Island, Bahamas. (M.Sc. Thesis)University of Geneva, Geneva, Switzerland (103 pp.).
- Waelbroeck, C., Labeyrie, L., Michel, E., Duplessy, J.C., McManus, J.F., Lambeck, K., Balbon, E., Labracherie, M., 2002. Sea-level and deep-water temperature changes derived from benthic foraminifera isotopic records. Quaternary Science Reviews 21, 295–305.
- Wainer, K.A.I., Rowe, M.P., Thomas, A.L., Mason, A.J., Williams, B., Tamisiea, M.E., Williams, F.H., Düsterhus, A., Henderson, G.M., 2017. Speleothem evidence for MIS 5c and 5a sea level above modern level at Bermuda. Earth and Planetary Science Letters 457, 325–334
- Ward, W.C., 1973. Influence of climate on the early diagenesis of carbonate eolianites. Geology 1, 171–174.
- Ward, W.C., 1975. Petrology and diagenesis of carbonate eolianites of Northeastern Yucatan Peninsula, Mexico. In: Wantland, K.F., Pusey III, W.C. (Eds.), Belize Shelf - Carbonate Sediments, Clastic Sediments, and Ecology. AAPG Studies in Geology2, pp. 500–571 (Tulsa, OK, USA).
- Ward, W.C., Vacher, H.L., 1997. Geology of coastal islands, Northeastern Yucatan Peninsula. In: Quinn, T.M. (Ed.), Geology and Hydrogeology of Carbonate Islands. Developments in Sedimentology54. Elservier, Amsterdam, NL, pp. 141–160.
- Whitacre, K., Kaufman, D.S., Kosnik, M.A., Hearty, P.J., 2017. Converting A/I values (ion exchange) to D/L values (reverse phase) for amino acid geochronology. Quaternary Geochronology 37, 1–6.
- White, B., Curran, H.A., 1995. Entombment and preservation of Sangamonian coral reefs during glacioeustatic sea-level fall, Great Inagua Island, Bahamas. In: Curran, H.A., White, B. (Eds.), Terrestrial and Shallow Marine Geology of the Bahamas and Bermuda. Geological Society of America Special Paper300, pp. 51–61 (Boulder, CO, USA).
- Wilber, R.J., Milliman, J.D., Halley, R.B., 1990. Accumulation of bank-top sediment on the western slope of Great Bahama Bank: rapid progradation of a carbonate megabank. Geology 18, 970–974.
- Wright, V.P., 1994. Paleosols in shallow marine carbonate sequences. Earth Science Reviews 35, 367–395.
- Yanes, Y., Romanek, C.S., 2013. Quaternary interglacial environmental stability in San Salvador Island (Bahamas): a land snail isotopic approach. Paleogeography, Paleoclimatology, Paleoecology 369, 28–40.
- Zhuravleva, A., Bauch, H.A., 2018. Last interglacial ocean changes in the Bahamas: climate teleconnections between low and high latitudes. Climate of the Past 14, 1361–1375.